

1 **Chance and predictability in evolution: the genomic basis of convergent**
2 **dietary specializations in an adaptive radiation**

3 Joel Vizueta¹, Nuria Macías-Hernández^{2,3}, Miquel A. Arnedo⁴, Julio Rozas^{1*} and Alejandro
4 Sánchez-Gracia^{1*}

5

6 ¹Departament de Genètica, Microbiologia i Estadística, and Institut de Recerca de la
7 Biodiversitat (IRBio), Facultat de Biologia, Universitat de Barcelona, Diagonal 643, 08028,
8 Barcelona, Spain.

9 ²Laboratory for Integrative Biodiversity Research, Finnish Museum of Natural History,
10 University of Helsinki; PO Box 17, 00014 Helsinki, Finland.

11 ³Island Ecology and Evolution Research Group, Instituto de Productos Naturales y
12 Agrobiología (IPNA-CSIC). C/Astrofísico Francisco Sánchez 3. La Laguna, Tenerife, Canary
13 Islands, 38206, Spain

14 ⁴Departament de Biologia Evolutiva, Ecologia i Ciències Ambientals and Institut de Recerca
15 de la Biodiversitat (IRBio), Facultat de Biologia, Universitat de Barcelona, Diagonal 643,
16 08028, Barcelona, Spain

17

18 * Corresponding authors. E-mail: jrozas@ub.edu, elsanchez@ub.edu

19

20

21

22 **Abstract**

23 The coexistence of multiple eco-phenotypes in independently assembled communities makes
24 island adaptive radiations the ideal framework to test convergence and parallelism in
25 evolution. In the radiation of the spider genus *Dysdera* in the Canary Islands, species
26 diversification occurs concomitant with repeated events of trophic specialization. These
27 dietary shifts, to feed primarily on woodlice, are accompanied by modifications in
28 morphology (mostly in the mouthparts), behaviour and nutritional physiology. To gain
29 insight into the molecular basis of this adaptive radiation, we performed a comprehensive
30 comparative transcriptome analysis of five Canary Island *Dysdera* endemics representing two
31 evolutionary and geographically independent events of dietary specialization. After
32 controlling for the potential confounding effects of hemiplasy, our differential gene
33 expression and selective constraint analyses identified a number of genetic changes that could
34 be associated with the repeated adaptations to specialized diet of woodlice, including some
35 related to heavy metal detoxification and homeostasis, the metabolism of some important
36 nutrients and venom toxins. Our results shed light on the genomic basis of an extraordinary
37 case of dietary shift convergence associated with species diversification. We uncovered
38 putative molecular substrates of convergent evolutionary changes at different hierarchical
39 levels, including specific genes, genes with equivalent functions, and even particular amino
40 acid positions. This study improves our knowledge of rapid adaptive radiations and provides
41 new insights into the predictability of evolution.

42

43 **Keywords:** Oceanic islands, Spiders, Diet specialization, Comparative transcriptomics,
44 Differential gene expression, Positive selection, Heavy metals, Toxins, Phenotypic
45 convergence

46

47 **Introduction**

48 The current limited knowledge of the evolutionary mechanisms underlying diversification
49 compromises our ability to manage and conserve biodiversity (Mergeay & Santamaria,
50 2012). Evolutionary biology provides a unifying conceptual framework to successfully
51 identify key diversification drivers through the study of molecular variation. As many other
52 fields, evolutionary biology has fully entered the genomics era, which opens up the
53 possibility of tackling longstanding questions regarding biodiversity in a more fruitful way
54 and at a lower cost (Losos et al., 2013). Although often seen as a gradual process that requires
55 the action of different evolutionary forces acting steadily over long periods of time (Coyne &
56 Orr, 2004), speciation can be very rapid under unstable environmental and ecological
57 conditions. In fact, one of the most promising approaches to disclose the relative impact of
58 these driving forces is the study of species radiations in nature, i.e., the rapid appearance of a
59 high number of species from a single common ancestor (Schluter, 2000). In adaptive
60 radiations, such as the classic examples of Darwin's finches (Almén et al., 2016) and the
61 cichlids in the great lakes of Eastern Africa (Henning & Meyer, 2014), significant
62 morphological differences appear over short periods of time despite the low levels of genetic
63 divergence accumulated at the genomic level. Nevertheless, the relative role of natural
64 selection and of other non-adaptive forces in such relevant evolutionary processes is a matter
65 of scientific debate (Muschick, Indermaur, & Salzburger, 2012).

66

67 Oceanic islands are considered natural laboratories for studying evolution. The entire biota of
68 these islands is derived from a few initial colonization events followed by local
69 diversification, which generates high levels of endemism and ecomorphological
70 differentiation (MacArthur & Wilson, 1967; Mayr, 1942; Whittaker & Fernández-Palacios,
71 2007). Thus, the biota of oceanic islands can be interpreted as the result of successful

72 independent evolutionary experiments starting with a single or multiple colonization events
73 from the continent (Emerson, 2002). The comparative analysis of such independent events
74 and the subsequent island radiation (both within and between islands) in different
75 archipelagos provides new insights into the general evolutionary process generating
76 biological diversity (Gillespie & Roderick, 2002; Losos & Ricklefs, 2009). Such
77 approximation has been successfully applied in a number of studies on oceanic islands
78 (Losos, Jackman, Larson, Queiroz, & Rodriguez-Schettino, 1998; Stroud & Losos, 2016),
79 such as Hawaii (Gillespie, 2004), the Galapagos (Grant & Grant, 2008) and the Canary
80 Islands and Madeira archipelagos (Juan, Emerson, Oromí, & Hewitt, 2000; Machado,
81 Rodríguez-Expósito, López, & Hernández, 2017), where explicit hypotheses on the
82 evolutionary processes underlying radiations have been tested.

83

84 The radiation of the genus *Dysdera* Latreille, 1804 (Araneae: Dysderidae) in the Canary
85 Islands is one of the most spectacular examples of island species diversification within
86 spiders (Arnedo, 2001; Arnedo, Oromí, Múrria, Macías-Hernández, & Ribera, 2007). As
87 many as 47 endemic species of this species-rich Mediterranean genus (approximately 250
88 species) have been reported in the Canary Islands (Macías-Hernández, López, Roca-Cusachs,
89 Oromí, & Arnedo, 2016; World Spider Catalog, 2019). The spiders of the genus *Dysdera* are
90 active nocturnal hunters that spend the daytime in silk retreats and are usually found under
91 stones, dead logs or leaf litter or even living in caves (Arnedo et al., 2007). This genus stands
92 out among spiders in having evolved trophic specialization; i.e., several species have been
93 shown to feed preferably (facultatively or even obligatorily) on terrestrial woodlice
94 (Crustacea: Isopoda) (Řezáč & Pekár, 2007; Řezáč, Pekár, & Lubin, 2008), a prey rejected by
95 most generalist predators (Pekár, Líznavá, & Řezáč, 2016). Available evidence suggests
96 that prey specialization (i.e., stenophagy) has appeared several times, both on the continent

97 and on the islands. Interestingly, the morphology of mouth parts predicts both dietary
98 preferences and capture strategy (chelicerae used as pincers, forks or keys) and the frequency
99 of captures among the specialists (Řezáč et al., 2008). All cheliceral types observed in
100 continental species have also evolved repeatedly in the Canary Islands, suggesting that prey
101 segregation is a major driving force of the spectacular diversification of the genus on the
102 islands (Arnedo et al., 2007). Woodlice are a difficult prey for other arthropods because of
103 their morphological, chemical and behavioural defences (Gorvett, 1956; Sutton, 1980). These
104 defences comprise dorsally protective armour, gland secretions producing repulsive odours,
105 indigestibility to many predators, and behavioural patterns such as nocturnal activity, rolling
106 into a ball or adhering to surfaces when threatened (Schmalfuss, 1984; Sutton, 1980). In
107 addition, these organisms accumulate high concentrations of heavy metals from the soil,
108 making them even more toxic to predators (Drobne, 1997). Consequently, woodlice are rarely
109 eaten by generalist predators. Within arthropods, only spiders and ants have developed
110 specialized strategies to feed on this prey (Dejean, 1997; Pekár et al., 2016). Nevertheless,
111 despite all this morphological and experimental evidence, the genetic basis of this remarkable
112 adaptation is completely unknown.

113

114 Moreover, the study of the molecular basis of such an extraordinary phenotypic convergence
115 offers an opportunity to address the question of predictability and repeatability of the
116 evolutionary process. Given that it is not possible to rerun the tape of evolution, the study of
117 parallel evolutionary outcomes in different scenarios provides a fairly good framework to
118 ascertain both to what extent similar molecular solutions has been exploited repeatedly, and
119 which aspects are predictable at different hierarchical levels (i.e., at the nucleotide, gene,
120 pathway or function level). Among *Dysdera* spiders, the specialized woodlice eaters (i.e.,
121 oniscophagous species) possess, in addition to the morphological modifications of chelicera,

122 important behavioural and nutritional adaptations to feed on isopods (Hopkin & Martin,
123 1985; Řezáč & Pekár, 2007; Toft & Macías-Hernández, 2017). With the aim of
124 understanding the genetic basis of these specific adaptations and to shed some light on the
125 longstanding debate of how predictable is molecular evolution, we designed a case study that
126 included adult individuals from two pairs of recently diverged endemic specialist-generalist
127 species from the Canary Islands, likely representing two phylogenetically and geographically
128 independent dietary shifts from a generalist ancestor. Our survey included the GV pair:
129 *Dysdera gomerensis* Strand, 1911 (El Hierro) and *D. verneaui* Simon, 1883 (Tenerife), the
130 TB pair: *D. tilosensis* Wunderlich, 1992 and *D. bandamae* Schmidt, 1973 (Gran Canaria),
131 and a third generalist endemic species external to both pairs: *D. silvatica* (La Gomera)
132 (Arnedo pers. Comm; Macías-Hernández, Oromí, & Arnedo, 2008; Vizueta et al., 2017),
133 which was used as an outgroup (Figure 1). We compared the transcriptome profiles and the
134 selective constraint patterns between specialists and generalists to identify the genomic
135 regions responsible for the rapid dietary adaptation of *Dysdera* species in the Canary Islands.
136 We studied transcriptomic data from adult individuals, we were able to detect putative
137 adaptive changes associated with food detection and assimilation, including its digestive and
138 metabolic aspects. True homoplasy can arise by evolving the same (or similar) trait from
139 either a non-shared common ancestor (convergent evolution) or a shared ancestor but through
140 evolutionarily independent events (parallel evolution). Here, we will refer to both cases with
141 the general term of “convergence”. We aimed to detect those evolutionary changes required
142 to explain a repeated character state in the two specialist lineages, either a gene expression
143 profile or a selective constraint pattern, matching phenotypic convergence. Nevertheless, both
144 incomplete lineage sorting of (ILS; Maddison, 1997) and species hybridization can produce
145 fundamental discordances between gene trees and the species tree, a phenomenon commonly
146 referred to as “hemiplasy” (Avice & Robinson, 2008), giving rise to the illusion of homoplasy

147 and the erroneous inference of convergence (Mendes, Hahn, & Hahn, 2016; Wu, Kostyun,
148 Hahn, & Moyle, 2018).

149

150 Here, and after controlling for the potential confounding effects of hemiplasy, we identified
151 clear signals of homoplasy at different hierarchical levels likely attributable to adaptive
152 convergence in specialist species. Noticeably, we even find signals of this adaptive process at
153 the amino acid level. The repeated changes matching phenotypic convergence found in this
154 study mostly affected genes and gene functions associated with the strategy of detoxifying
155 heavy metals (and perhaps other toxic substances) accumulated by woodlice, to the enhanced
156 assimilation of some nutrients and, to a lesser extent, to venom composition.

157

158 **Material and Methods**

159 **Study design and sample materials**

160 Our study design included two pairs of phylogenetically related *Dysdera* species endemic
161 from the Canary Islands. Each pair of close relatives was composed of a generalist and a
162 specialist (stenophagous) species regarding their diet and shared a generalist ancestor, which
163 implies that at least two specialization events occurred independently during the divergence
164 of these four species, one on each species pair (Figure 1). Both the phylogenomic analysis
165 performed here and recent multi-locus based phylogenies including other endemic species of
166 this genus (Arnedo et al. unpublished results) indicate that *D. gomerensis* and *D. verneaui* are
167 true sister taxa, while *D. tilosensis* and *D. bandamae* are very closely related, although it is
168 difficult to know if they are each other closest relatives. Similarly, the ancestral state
169 reconstruction supports that the ancestor of the complete Canarian radiation was a generalist,
170 while *D. tilosensis* is a derived specialist from a generalist ancestor. For the case of *D.*
171 *gomerensis* this is much more difficult to establish because of the phylogenetic uncertainty,
172 probably due to a very rapid radiation of these species group. In any case, this rapid radiation
173 however makes that most candidate changes in the *D. gomerensis* lineage (see below), would
174 be adaptations to stenophagy, independently of whether the ancestor was a complete
175 generalist, or just a facultative intermediate.

176

177 The two specialists species of our study show modifications in their mouthparts that have
178 been associated with a preference for using isopods as a prey (Řezáč et al., 2008; Macías-
179 Hernández et al, in prep) (see Figure 1). We collected 16 individuals of *Dysdera tilosensis*
180 (10 males and 6 females) and 14 individuals of *D. bandamae* (5 males and 9 females) in Gran
181 Canaria, and 12 males of *D. verneaui* in Tenerife and 15 females of *D. gomerensis* in El
182 Hierro (Table S1). We also included in the analysis a fifth Canary Island endemic *Dysdera*

183 species, the generalist *D. silvatica*, as an outgroup and to polarize the evolutionary changes in
184 internal branches (Vizueta et al., 2017) (Figure 1).

185

186 **Transcriptomic analysis**

187 For each species, we sequenced the transcripts from the palps (*PALP*), the first pair of legs
188 (*LEG#1*), all other legs (*LEG#234*), and the rest of the body (*REST*), separately in four
189 different RNAseq experiments. We applied this strategy to maximize the detection of low
190 expressed genes, especially chemosensory gene family members in spider appendices (see
191 Vizueta et al., 2017 and Frías-López et al., 2015; Supplementary Methods). Specimens were
192 starved for two weeks at the laboratory and posteriorly fixed in liquid nitrogen and stored at
193 -80°C until further processing. From the total RNA, we sequenced the transcriptomes in the
194 Illumina HiSeq 4000 platform using pair-end libraries (100-bp reads; Table S1). A detailed
195 description of raw data pre-processing, transcriptome assembly and functional annotation of
196 the transcripts from the four species is available in Supplementary Methods.

197

198 **Species-tree, gene-tree discordance, and risk of hemiplasy**

199 We identified all groups of homologous genes that share at least one member in the ancestor
200 of the five *Dysdera* species (i.e., orthology groups) using OrthoMCL with default parameters
201 (Li, Stoeckert, & Roos, 2003). We further separated single-copy orthologs from multigene
202 families. Since at the moment of starting this work, all published phylogenetic analyses
203 including the studied species were based on few genes (Arnedo, 2001; Arnedo et al., 2007),
204 we performed a more comprehensive phylogenomic analysis using all single copy orthologs
205 across the five Canarian *Dysdera* species plus *D. crocata* Koch, 1839 (the phylogenetically
206 closest continental species of this genus with available transcriptome data; Fernández,
207 Hormiga, & Giribet, 2014) (Figure 2). Only complete or nearly complete transcripts free of

208 premature stop codons were included in the analysis. The multiple sequence alignments
209 (MSA) of the CDS of each orthology group were generated with the program T-Coffee
210 (Notredame, Higgins, & Heringa, 2000) and further concatenated in a single MSA using in
211 house Perl scripts. We set the GTRGAMMA substitution model in a partitioned scheme to
212 obtain the maximum likelihood (ML) tree in the software RAxML (Stamatakis, 2014). Model
213 parameters were estimated independently for each single-copy ortholog and node support was
214 obtained after 500 bootstrap replicates.

215

216 We approximated the divergence times between the five Canarian *Dysdera* species by fitting
217 the data from single copy orthologs to the unrooted tree topology of the ML tree after
218 excluding *D. crocata*. We set the same substitution model and partition scheme than in the
219 previous RAxML analysis. We used the penalized likelihood method of Sanderson (2002),
220 implemented in the program r8s v1.80, to generate the ultrametric tree and to estimate node
221 ages (Sanderson, 2003). We set a calibration point in the node representing the split of the *D.*
222 *silvatica* lineage from the rest of lineages (3.4-7.8 Mya range; Macías-Hernández, Bidegaray-
223 Batista, Emerson, Oromí, & Arnedo, 2013).

224

225 We also inferred a species tree that incorporates gene-tree uncertainty using ASTRAL
226 (Zhang, Rabiee, Sayyari, & Mirarab, 2018). For that, we first estimated the ML tree of each
227 individual MSA (i.e., a gene tree for each single-copy ortholog) with RAxML (setting the
228 GTRGAMMA substitution model and calculating node support with 1000 bootstrap
229 replicates). Moreover, we estimated the Hemiplasy Risk Factor (HRF) along the phylogeny
230 using the PePo package (Guerrero & Hahn, 2018). For the analysis, we used the species tree
231 inferred with ASTRAL (with branch lengths in $2N_e$ generation units), a very approximate
232 estimate of the population scaled mutation rate in *D. silvatica* ($\theta = 0.011$; estimate obtained

233 from a short read alignment to the first genome draft of this species; Sánchez-Herrero et al.,
234 2019), a generation time of 1.5 years, and six different effective population sizes, N_e (10^3 , $5 \times$
235 10^3 , 10^4 , 5×10^4 , 10^5 and 10^6). Finally, all candidate genes exhibiting resolved discordant
236 topologies (i.e., with bootstrap support $\geq 75\%$ in at least one node producing discordance
237 with the species tree) were excluded for the downstream functional prediction analyses and
238 their interpretation. Finally, we used the D_{FOIL} statistic (Pease & Hahn, 2015) to test for
239 introgression between the specialist lineages in presence of ILS, using both *D. silvatica* or *D.*
240 *crocata* as outgroups.

241

242 **Differential expression analyses**

243 Differential expression (DE) analyses were performed separately in each generalist-specialist
244 pair (GV and TB pairs; see Figure 1; Supplementary Methods). Raw reads of the RNAseq
245 from each species and body part were mapped back to their own reference CDS and to the
246 CDS of the other species in the pair by using BOWTIE2 version 2.2.3 (Langmead &
247 Salzberg, 2012). Read counts and TMM-normalized FPKMs (i.e., trimmed mean of log-
248 expression ratios-normalized fragments per kb of exon per million reads mapped) were
249 estimated for single-copy genes and multigene families using RSEM 1.2.19 software (Li &
250 Dewey, 2011). To test for genes showing DE between specialists and generalist species, we
251 calculated the negative binomial dispersion of read counts across species pairs of a set of
252 housekeeping (HK) genes with EdgeR version 3.18.1 (Robinson, McCarthy, & Smyth, 2010).
253 We used this dispersion to conduct the DE analysis between specialist and generalist species.
254 We merged all body parts (within a species) to homogenize the differences in the number of
255 REST samples between species pairs. To avoid type I and II errors associated to this merging,
256 especially when gene expression is higher in *REST* relative to legs (both *LEG#1* and
257 *LEG#234*) and *PALP*, we used total read counts from all samples normalized for each library

258 size to perform differential expression analyses. The P -values of these analyses (one per
259 gene) were corrected for the false discovery rate (Benjamini & Hochberg, 1995) (FDR). We
260 considered that a gene is differentially expressed between two species when expression levels
261 are significantly different with a $FDR < 0.05$.

262

263 **Selective constraints analyses**

264 We used the adaptive Branch-Site Random Effects Likelihood (aBSREL) model
265 implemented in the HyPhy package (Pond, Frost, & Muse, 2005; Smith et al., 2015) to test if
266 positive selection has occurred repeatedly in the same gene in specialist lineages. This
267 method is based on the parameter ω (the ratio of nonsynonymous (d_N) to synonymous (d_S)
268 substitution rates, $\omega = d_N/d_S$) and allows fitting an optimal number of ω classes to codon
269 sequence alignments of single-copy orthologs in each branch of the phylogeny (Figure 2;
270 Supplementary Methods). Positive selection is inferred when a gene shows codons fitting a
271 class with $\omega > 1$ in a particular lineage. We also tested for relaxation or intensification of the
272 strength of natural selection in these single copy orthologues in specialist lineages using the
273 RELAX framework in HyPhy (Wertheim, Murrell, Smith, Kosakovsky Pond, & Scheffler,
274 2015). Besides, we applied the Mixed Effects Model of Evolution (MEME) implemented in
275 the HyPhy package (Murrell et al., 2012) to identify individual sites evolving under episodic
276 positive selection (in one or more lineages) in the set of candidates from PCOC analysis (see
277 below). Both methods are based on the same principle of aBSREL of fitting different
278 probabilistic models of the ω parameter distribution, and also inferred positive selection
279 when $\omega > 1$. Finally, we applied the aBSREL model to test for episodic positive selection
280 acting on gene families in specialist lineages. In this case, we used the same workflow as for
281 the single copy orthologs but applying the FastTree program (Price, Dehal, & Arkin, 2010) to
282 approximate a ML tree of each family.

283

284 Convergent amino acid evolution

285 To detect convergent amino acid evolution in specialist lineages, we aligned the amino acid
286 sequences of the PS candidates using the software PRANK and applied the method PCOC
287 (Rey, Guéguen, Sémon, & Boussau, 2018) (Profile Change with One Change), a recently
288 developed approach to identify convergent shifts in the amino acid substitution rate across a
289 phylogeny, to each individual MSA. Moreover, we used computer simulations to test the
290 performance of PCOC method with our empirical data. We applied the same species tree,
291 average sequence length and model parameters set in the PCOC analysis of the observed data
292 to simulate sequences both with convergent (2% of sites undergoing convergent amino acid
293 substitutions) and without convergent changes (Rey et al., 2018). Using these simulated
294 sequences, we estimated the false discovery rate (FDR; using simulations without
295 convergence) and true positive rate (TPR; using simulations with convergent amino acid
296 substitutions) associated with this analysis.

297

298 GO enrichment

299 We used R and GOstats (Falcon & Gentleman, 2007) to carry out the gene ontology (GO)
300 enrichment analysis and REVIGO (Supek, Bošnjak, Škunca, & Šmuc, 2011) to generate a
301 graphical representation of the results. We also used Blast2GO suite (Conesa et al., 2005) to
302 identify KEGG pathways enriched in the list of candidates (Kanehisa & Goto, 2000).
303 Hypergeometric tests were performed with dhyper function of the R package STATS.

304

305 **Results**

306

307 We constructed 16 RNA-seq datasets (four different body parts in four species) to obtain four
308 new complete *Dysdera* transcriptomes (Table S1). As expected, both the number of species-
309 specific transcripts (from 170,846 to 347,878) and the number of functionally annotated
310 genes differed between species (Table 1), but the transcriptome completeness, measured as
311 the number and integrity of CEG genes, was quite similar (Table S2). Only 30% of the
312 transcripts encoded protein-coding genes; the rest corresponded to either non-coding
313 transcripts or assembly artefacts (Table 1). Furthermore, ~35% of the predicted proteins
314 showed no significant sequence similarity or conserved profiles with known arthropod genes
315 (i.e., putative orphan genes of the *Dysdera* lineage). Among the annotated proteins, most
316 were chelicerate specific, and ~66% of the top BLAST hits matched spider sequences (Figure
317 S1).

318

319 We identified a total of 13,947 orthologous groups across the five Canarian *Dysdera* species,
320 of which 7,958 were free of premature stop codons, and 4,539 showed complete sequences in
321 all species (Figure 2). The number of single-copy orthologues across the five species was
322 9,473, a number that increased to 19,497 in the GV pair and 24,212 in the TB pair (Table S3).
323 The maximum likelihood (ML) tree that included *D. crocata* (2,472 genes; 2,926,723 bases)
324 confirmed the expected phylogenetic relationships (Figure 1), i.e., that *D. silvatica* is sister to
325 the two generalist/specialist sister lineages (GV and TB). We estimated that *D. gomerensis*
326 and *D. verneau* diverged approximately ~4.1 Mya, whereas the split between *D. tilosensis*
327 and *D. bandamae* occurred ~3.1 Mya; the age of the common ancestor of these four lineages
328 dates to ~4.5 Mya (analysis based on 4,539 genes; Figure 1). These estimates are similar to
329 those obtained in Macías-Hernández et al., (2013).

330

331 These very recent divergence times, especially the short internal branch lengths, indicated
332 that hemiplasy might represent an important confounding factor in our inferences of
333 convergent evolution. Indeed, although the species tree estimated with ASTRAL had the
334 same fully supported topology (the local posterior support for each branch was 1) than as the
335 ML tree based on the concatenated MSA, the final normalized quartet score of this species
336 tree (0.65) uncover a high gene tree conflict in our data set. The risk of hemiplasy (HRF)
337 estimated along the species tree obtained with ASTRAL, varied according to the effective
338 population sizes and the examined branch (Figure 3), being small for $N_e \leq 10^4$, high in
339 branches A and C for $N_e \geq 10^5$, and extremely high in all branches for $N_e \geq 10^6$. Given the
340 high fraction of discordant gene trees observed in our data (5,275 out of 7,784 gene trees;
341 3,666 with high bootstrap support ≥ 0.75 in at least one discordant node) together with HRF
342 estimates, the surveyed species (and their ancestors) would have intermediate to high
343 effective population sizes, in a range of $10^4 < N_e \leq 10^6$. Although only a small fraction of
344 these inconsistencies might really affect our inferences of homoplasy (see discussion), we
345 specifically considered this confounding factor in our study. In contrast, we did not detect the
346 characteristic hallmark of gene flow between extant specialist lineages in the D_{FOIL} analysis
347 of transcripts, neither by analyzing all transcripts separately nor concatenating them in
348 different gene groups (i.e., all transcripts, all candidates, only gene expression, or only
349 positive selection candidates; results not shown; see below for the precise definition of each
350 type of candidate).

351

352 **Gene expression changes matching phenotypic convergence: individual gene level**

353 Despite the sex-ratio bias of the studied samples (Table S1), the PCA analysis of the eight
354 *REST* samples of the specialist *D. tilosensis* sequenced separately (four males and four
355 females), showed no evidence of sex-specific expression (Figure S2), which is in agreement

356 with the absence of morphological dimorphism between sexes reported for the Eastern
357 Canarian clade of this genus (Macías-Hernández et al., 2008). We found 774 (out of 19,497)
358 and 1,044 (out of 24,212) genes showing differential expression between specialists and
359 generalist species in the GV and TB pairs, respectively (Figure S3; Table S4). Remarkably,
360 147 genes (out of 193) had patterns of gene expression matching phenotypic convergence,
361 i.e., the expression profiles had the same trend in both species' pairs with the two specialists
362 significantly under- or overexpressed (hereafter referred to as Matching Gene Expression
363 "MGE" candidates); however, in three cases the tree showed discordant genealogies
364 supported by the entire transcript sequence. The final number of MGE candidates (144 genes)
365 is much higher than that expected by a neutral model of gene expression evolution, both
366 when considering all differentially expressed genes (hypergeometric test; $P = 1.3 \times 10^{-67}$) and
367 separating genes over- or underexpressed in specialist lineages ($P = 2.3 \times 10^{-14}$ and $P = 4.2 \times 10^{-121}$,
368 respectively; hypergeometric test). The proportion of genes significantly underexpressed
369 in specialists was higher both in the two species pairs considered separately (68% in GV and
370 61% in TB) and, to a much greater extent, across the 144 shared DE candidate genes (114
371 genes; 79%) (Figure 4; Table S4). All MGE candidates except two functionally
372 uncharacterized proteins (OG9619 and OG15050 in *PALP*) and one phosphatase (OG1641 in
373 *LEGS*), were predominantly expressed in *REST*, (Figure 4; Figure S3), and none of them
374 show DE between males and females of *D. tilosensis* in this body part (results not shown).
375 All these findings indicate that DE analyses are reflecting real differences between specialist
376 and generalist species, and not sex or body part-specific features. Yet, we cannot completely
377 rule out that some of the uncovered candidates ~~was-were a~~-false positives, so they should be
378 considered as promising candidates to be further validated.

379

380 Within the biological processes significantly overrepresented (Figure 5a) among MGE
381 candidates, we identified genes involved in the homeostasis of metal ions; catabolism of
382 amino acids, sugars and chitin and activities of enzymes such as phosphatase and hydrolase.
383 The separate analysis according to the direction of gene expression change showed that the
384 114 MGE candidates downregulated in specialists are significantly enriched in assembly and
385 organization of chromatin, cytoskeleton and other cellular structures (such as the organelles),
386 potential regulation of developmental processes through the smoothed pathway, cell
387 morphogenesis and growth processes, and catabolism of sugars and amino acids. In contrast,
388 the 30 MGE candidates upregulated in specialists are significantly enriched in GO terms
389 associated to the metabolism of steroids, lipids and dicarboxylic acid, the activities of
390 phosphatases and hydrolase, the membrane transport of different substances, and responses to
391 various external stimuli including cellular response to oxidative stress. Other interesting but
392 not GO-enriched functions of the MGE candidates include iron ion binding (a predicted
393 cytochrome P450 protein overexpressed in specialist spiders) and zinc ion binding (mostly
394 represented by various putative zinc finger-containing proteins; Table S4). Furthermore, we
395 also found two putative venom toxins among the 144 MGE candidates, one of which encodes
396 a protein similar to the α -latrocrustatoxin (underexpressed in specialists), while the other is an
397 U32-aranetoxin-Av1a overexpressed in specialists (see Figure S4 and Table S4 for a more
398 detailed functional description of the MGE candidates, including significantly enriched
399 molecular functions).

400

401 Our analysis also detected 21 genes specifically expressed in specialists (i.e., with no
402 detectable expression in generalists; referred to as Matching Specialist-specific Expression
403 “MSE” candidates) (Figure 2). Fifteen of these MSE candidates encode proteins with no
404 significant sequence similarity with any entry in the searched databases; the other six cases,

405 which were not enriched in any GO term, encode catalytic activities, such as hydrolases and
406 peptidases, or are associated with zinc ion-binding proteins, likely involved in the regulation
407 of gene expression (Table S4).

408

409 The highly fragmented nature of the transcripts encoding members of the major
410 chemosensory gene families (Vizueta et al., 2018) prevented the credible assignment of many
411 orthogroups and, therefore, a reliable DE analysis comparing specialists and generalists.
412 Besides, for the few orthogroups that could be assigned, we did not find any concordant DE
413 pattern in specialists. The same negative results were obtained for the other orthogroups that
414 showed DE in the chemosensory appendages (*PALP* and *LEG#1* and *LEG#234*) in the study
415 of Vizueta et al., (2017).

416

417 **Gene expression changes matching phenotypic convergence: gene function level**

418 Apart from the 144 MGE candidates, the group of genes with DE only in one species pair,
419 627 in GV pair and 897 in TB pair, respectively, also shared a significant number of enriched
420 GO terms (70 terms; hypergeometric test, $P= 4.7 \times 10^{-11}$ for all DE genes; $P = 2.2 \times 10^{-23}$ and P
421 $= 1.3 \times 10^{-2}$ for under- and overexpressed genes, respectively). Remarkably, some of these GO
422 terms are the same as those overrepresented among the MGE candidates. For the genes
423 underexpressed in specialists, these included chromatin assembly, the organization of cellular
424 components, such as the cytoskeleton or organelles, and cell growth. Other additional
425 functions, such as phosphate metabolism regulation and the apoptotic process involved in
426 morphogenesis, are also shared among these genes. For the genes overexpressed in
427 specialists, the enriched functions shared between species pairs include lipid catabolism,
428 oxidation-reduction process and response to antibiotics (Figure S4 and Table S4).

429

430 Among the orthogroups with DE only in one species pair but with equivalent functions, we
431 found genes involved in detoxification processes and genes encoding various members of the
432 cytochrome P450 family (most of them overexpressed in specialists, seven and nine different
433 copies in the GV and TB pairs, respectively) or proteins with esterase activity (seven and six
434 of these enzymes in the GV and TB pairs, respectively). Additionally, we found 29 putative
435 venom toxin-encoding genes in the GV pair (eight overexpressed in G) and 34 in the TB pair
436 (26 overexpressed in T). Interestingly, although the encoding genes differed between the two
437 specialists, they had very similar predicted functions, such as astacin-like metalloprotease
438 toxin precursors or aranetoxin-Av1a and latrotoxins, among others (Table S4).

439

440 **Positive selection matching phenotypic convergence: individual gene level**

441 We applied the aBSREL model to estimate the distribution of ω values of all single-copy
442 orthologues with complete sequences and without premature stop codons (7,784 genes;
443 Figure 2; Table S3). This genome-wide analysis uncovered opposite trends between GV and
444 TB pairs; while the overall selective constraints appear to have been relaxed in the *D.*
445 *tilosensis* lineage, they intensified in the *D. gomerensis* branch (Figure S5). Nevertheless, the
446 analysis of individual genes identified nine genes with significant differences in the selective
447 constraint values shared between the two specialists (or the two generalists) (RELAX
448 framework analysis, FDR of 0.2; Table S5; referred as Matching Functional Constraint
449 “MFC” candidates). Six of these candidates showed the relaxation hallmark in specialists,
450 while the other three showed a significant increase in the selective constraint. We found some
451 overrepresented biological functions among MFC candidates, such as carbohydrate
452 metabolism and homeostasis, neuropeptide signaling, tRNA modification and pyridine
453 metabolism (Figure S4). When we considered not enriched GO terms, the genes with
454 increased functional constraints in specialists encode proteins similar to the membrane

455 glycoprotein *LIG-1*, a neuropeptide receptor-like protein, and zinc finger proteins while the
456 genes that have relaxed most in specialist's species encode two zinc finger-like proteins and a
457 hexokinase.

458

459 We identified 297 genes with significant evidence of positive selection in specialist lineages,
460 169 in *D. gomerensis*, 150 in *D. tilosensis* and, remarkably, 22 cases in which positive
461 selection was inferred in both dietary specialists (Figure 2; Table S6; referred to as Matching
462 Positive Selections "MPS" candidates). After excluding five coding regions with discordant
463 genealogies supported by the entire transcript sequence, the number of MPS candidates (17)
464 is clearly greater than that expected by chance (across the 297 genes showing positive
465 selection in specialists; hypergeometric test; $P = 1.5 \times 10^{-8}$). These genes are enriched in
466 biological processes such as germ cell migration and cell death, cell junction assembly and
467 organization, regulation of the immune response or iron ion homeostasis (Figure 5; Figure
468 S4). Interestingly, one of these genes with endopeptidase inhibitor activity encodes a protein
469 with sequence similarity to U24-ctenitoxin-Pn1a, a possible venom toxin related to cysteine
470 proteinase inhibitors.

471

472 The PCOC method (Rey et al., 2018) identified convergent shifts in amino acid preferences
473 in 14 out of the 17 MPS candidates (FDR = 0.03%; TPR = 99.7%; Figure 6; Table S6; Figure
474 S6). Furthermore, in five cases, the subsequent MEME analysis indicated that some of the
475 amino acid sites involved in these convergent shifts have also evolved by positive selection (8
476 amino acid sites; Figure 6). The target genes include i) the U24-ctenitoxin-Pn1a candidate
477 toxin (OG6752 orthogroup; 6 amino acid changes); ii) OG7181, a transcript encoding a
478 protein similar to tectonin (10 amino acid changes, 3 of them under); iii) OG9641, a
479 transcript encoding a protein involved in response to oxidative stress (3 amino acid changes,

480 one of them also detected with MEME); iv) OG11255, a gene that encodes a product similar
481 to a mannose receptor (5 amino acid changes, 2 of them also detected with MEME); v)
482 OG13286, a protein likely encoding a sodium channel (1 amino acid change, also detected
483 with MEME); and vi) OG16682, a hydrolase involved in nitrogen compound metabolism (4
484 amino acid changes, one of them detected with MEME). The analysis also inferred some
485 amino acid substitutions responsible of a convergent shift of preferences in specialists but
486 without evidence of positive selection in OG9529, a putative dehydrogenase and
487 oxidoreductase (4 amino acids) (Figure S6).

488

489 **Positive selection matching phenotypic convergence: gene function level**

490 Although the group of genes under positive selection in only one of the two specialists (147
491 in GV pair and 138 in TB pair, respectively) did not share more significantly enriched GO
492 terms than expected by chance (only three shared GO were enriched in both pairs;
493 hypergeometric test; $P = 0.19$), the number of total GO terms shared by these two groups is
494 greater than expected ($P = 5.3 \times 10^{-75}$ based on the hypergeometric distribution). Among
495 shared GO terms, we found processes and functions such as chitin metabolism (including
496 proteolysis activity), lipid metabolism, metal ion binding (zinc in both pairs, copper in *D.*
497 *gomerensis* and iron in *D. tilosensis*), and hydrolase and oxidoreductase activities (Figure
498 S4). In addition, we also detected the signature of positive selection in six genes encoding
499 putative venom toxins: four in *D. gomerensis* and two in *D. tilosensis* (Table S6).

500

501 The gene family analysis also uncovered the hallmark of positive selection in five gene
502 families affecting both specialist lineages (Figure 2; Table S6). One family (the OG3133
503 orthologous group), which included sequences without any functional annotation, also
504 showed copy number variation in the two specialists (2 and 3 copies in *D. gomerensis* and *D.*

505 *tilosensis*, respectively, compared to one in the generalist species). The other four gene
506 families encoded proteins with possible functions in chitin metabolism and sequences similar
507 to carbohydrate and zinc ion-binding proteins, hydrolases and other enzymes with catalytic
508 activity. Again, we found a gene family encoding putative venom components (in this case,
509 with no characterized target) among positively selected gene families.

510

511 Discussion

512 The evolution of stenophagy, dietary specialization from a generalist ancestor, most likely
513 involves gene regulatory changes, amino acid replacements in proteins, and/or even copy
514 number variation in gene families. Here, we focused our analysis on the first two issues since
515 comparative transcriptomics based on *de novo* assemblies prevents accurate estimation of
516 changes in gene expression and gains and losses in gene family members. Our approach
517 allows detecting genetic changes in the genes expressed in adults (either in the same gene or
518 in equivalent gene functions) matching the phenotypic convergence observed in dietary
519 specialist *Dysdera*. Nevertheless, it is largely known that hemiplasy can also produce such
520 matching patterns, inducing false evidence of convergent evolution (Mendes et al., 2016; Wu
521 et al., 2018). Indeed, the high level of gene tree discordance caused by ancestral
522 polymorphisms could potentially explain some of the repeated changes identified in *D.*
523 *gomerensis* and *D. tilosensis*. Nonetheless, some lines of evidence support that most of the
524 candidates reported in this study accumulated convergent changes in specialist lineages. First,
525 for realistic effective population sizes (i.e., $10^4 < N_e \leq 10^5$; these spiders are island endemic
526 predators with likely low census sizes), the probability of observing discordant trees
527 matching the phenotypic convergence is very low (Figure 3). The estimates of the HRF
528 values in branch B under realistic effective population sizes ranged from 0.001 to 0.134
529 (Figure 3b and 3c). Therefore, the probability of occurrence of ILS on this branch,
530 accompanied by a mutation in the branch A or in an older lineage creating a false pattern of
531 homoplasy, is much lower than that of true homoplasy (Guerrero & Hahn, 2018). Second,
532 among the total set of discordant gene trees with high bootstrap support, only the 1.69% (62
533 out of 3,666) yielded resolved topologies that match exactly the one expected from
534 convergence in specialists, which agrees with hemiplasy risk predictions for intermediate
535 effective population sizes. Even so, and to be conservative, we excluded from the

536 downstream functional prediction analysis all candidates with gene trees included in this
537 1.69%. This approach, however, may not be suitable for detecting convergent changes in
538 gene expression in specialists. Actually, the assumption that the regulatory regions
539 responsible of the concordant changes in gene expression of candidate genes are completely
540 linked to the transcribed sequence (i.e., both share the same gene tree) may not be correct.
541 Estimates of the recombination rate in these genomes are not available and, more
542 importantly, some of these mutations could be far away from the coding region, even acting
543 in *trans*. In these cases, however, we would expect that gene-tree discordance will be
544 randomly distributed across the genome. We found, by contrast, a clear bias in our candidates
545 towards genes and functions biologically relevant for dietary specialists. Bearing all this in
546 mind, the fixation of convergent genetic changes remains as the most likely explanation for
547 most of the discordant patterns matching phenotypic convergence, even for MGE candidates.
548 Consequently, we demonstrated that our study design, with two evolutionary replicates of the
549 same dietary specialization event, was able to identify potential candidate genes and groups
550 of functionally equivalent genes responsible in part to these remarkable ecological shifts.
551
552 A priori, we would expect that the biological functions targeted by selection are related to
553 prey capture and food assimilation, both in digestive and metabolic aspects. Since genetic
554 changes underlying morphological modifications of the specialists' mouthparts likely involve
555 changes in gene expression patterns during development, they were undetectable in our
556 comparative analysis of adult transcriptomes. However, other aspects related to the detection,
557 attack, consumption and digestion of a prey with remarkable behavioural and chemical
558 defences definitely played a crucial role in specialization. Several studies have revealed
559 significant differences in the growth and nutrient extraction efficiencies in specialist *Dysdera*
560 fed on woodlouse, which suggests the existence of metabolic adaptations (Řezáč & Pekár,

2007; Toft & Macías-Hernández, 2017; Macías-Hernández et al., *in prep.*). Toxicity is the most relevant nutritional aspect that makes isopods a prey commonly rejected by most generalist spiders (Hopkin & Martin, 1985). Indeed, isopods accumulate toxic substances, including high concentrations of heavy metals from the soil, especially copper but also zinc, lead and cadmium, in vesicles such as lysosomes (Paoletti & Hassall, 1999). The toxic effects as well as some of the underlying genetic response mechanisms of heavy metals on terrestrial invertebrates have been known for a long time (Janssens, Roelofs, & van Straalen, 2009; Merritt & Bewick, 2017; Migula, Wilczek, & Babczyńska, 2013). Remarkably, our results are in full agreement with the few comparative transcriptomics studies conducted on these types of animals under different metal-stress conditions (e.g. Gomes, Scott-Fordsmand, & Amorim, 2014; Roelofs et al., 2009; Zapata, Tanguy, David, Moraga, & Riquelme, 2009), including in spiders (Li et al., 2016). These studies demonstrate that arthropods exposed to heavy metals show important gene expression changes relative to controls; remarkably, some of the reported gene targets also appear among our MGE candidates or correspond with some of the molecular functions enriched in our list. Some examples include ABC transporters, amiloride-sensitive sodium channels, ATPases, MAP kinases, ubiquitin ligases, histones, members of the cytochrome P450 family and ribosomal proteins (Table S4). These consistent results across different studies on phylogenetically distant species, support the idea of a relatively well-conserved common mechanism for the tolerance of heavy metal toxicity across animals. The old origin of such an evolutionary mechanism validates our approach for identifying the genetic determinants of stenophagy in *Dysdera*.

582

583 Genetic changes matching phenotypic convergence: metal-induced damage or adaptive
584 response to metal stress?

585 We found that most MGE candidates were specifically downregulated in specialists and
586 encoded molecular functions involved in cell response, vesicular transport, organization of
587 organelles and cytoskeleton, cilia assembly, or cell adhesion (Table S4). Noticeably, these are
588 the most frequent cell modifications observed in intestinal tissue damage by heavy metals
589 from the diet (e.g., Bednarska et al., 2016; Köhler & Alberti, 1992; Zhang et al., 2001).
590 Indeed, in soil arthropods subjected to heavy-metal stress, midgut cells show evident
591 histological modifications indicative of metal deposition in intracellular granules and gut
592 epithelial degeneration. Although the downregulation pattern observed in specialist *Dysdera*
593 could be the result of a direct stress-induced perturbation of gene expression caused by the
594 high concentration of heavy metals supplied in a woodlouse-rich diet, they might actually be
595 part of an adaptive biological response to excrete metals or other toxic substances more
596 efficiently, thus avoiding their assimilation (Van Straalen & Roelofs, 2005). Consistent with
597 this hypothesis, we observed concordant DE patterns in some MAP kinase pathway members,
598 which participate in an important stress-activated/immune response cascade (Chmielowska-
599 Bąk & Deckert, 2012), and in some ubiquitin ligases, which, among other functions, are
600 involved in the inhibition of cell growth and cycle arrest in response to DNA damage (Cao &
601 Yan, 2012). The adaptive response in specialists would consist of downregulating a set of
602 genes to keep gut epithelial cells in a semi-degenerated functional and structural state that
603 allows enhanced accumulation of heavy metals in granules and very fast and effective
604 intestinal exfoliation and regeneration.

605

606 Our analysis also uncovered a number of upregulated MGE and MPS candidates associated
607 with iron, copper and zinc binding and homeostasis, which can also be part of an adaptive
608 mechanism of detoxification in specialist *Dysdera*. Among these candidates, we found
609 amiloride-sensitive sodium channels, membrane ATPases and ABC and dicarboxylate

610 transporters. These proteins are either antiporters for metal cations or are involved in cellular
611 mechanisms for heavy metal vacuolar sequestration (Ahearn, Sterling, Mandal, &
612 Roggenbeck, 2010) or in cellular metal homeostasis and detoxification (e.g., Sooksa-Nguan
613 et al., 2009; Lee et al., 2014). Another set of interesting candidates are the proteins annotated
614 as syntaxin-5-like proteins with a SNARE domain, which are involved in vesicle tethering
615 and fusion associated with copper ion homeostasis (Norgate et al., 2010) and, in addition to
616 being significantly overexpressed in both specialists, also show signals of positive selection
617 in *D. tilosensis*.

618
619 It is well known that heavy metal-associated toxicity is largely due to damage to the oxidative
620 tissue caused by the accumulation of reactive oxygen species in the cell (Schieber & Chandel,
621 2014). Noticeably, among the upregulated MGE candidates (and those regulated in only one
622 of the specialists), we found members of family 3 of the P450 cytochromes, a group of
623 monooxygenases that constitute the largest and most functionally diverse class of insect
624 detoxification enzymes and that have been implicated in the oxidative detoxification of
625 furanocoumarins, alkaloids, plant secondary metabolites and synthetic insecticides (Nelson &
626 Nebert, 2011). Additionally, we identified among the candidates several esterases, a group of
627 proteins with a role in heavy metal and pesticide detoxification that have been used as
628 biomarkers of metal exposure in many organisms, including spiders (Wilczek, Babczyńska,
629 Migula, & Wencelis, 2003). We identified esterases significantly overexpressed in both
630 specialists, although in this case, the orthogroups of *D. gomerensis* and *D. tilosensis* were
631 different, suggesting possible convergence at the functional level rather than at the gene level.
632 Remarkably, two of these esterases also showed a positive selection signal in *D. gomerensis*.

633

634 We also detected other MGE candidates associated with the metabolism of some essential
635 nutrients, such as proteins with chitin-binding and chitinase activity, and enzymes involved in
636 the metabolism of amino acids, sugars and lipids. Given that most of these candidates were
637 downregulated in specialists, the adaptive advantage could be associated with a reduction in
638 biosynthetic processes to save energy, presumably to dedicate the energy to detoxification
639 processes. However, the presence of some upregulated and positively selected genes among
640 these metabolic candidates indicates that specialists might also have developed an adaptive
641 mechanism to enhance the assimilation and metabolization of some other nutrients present in
642 woodlice but less accessible to other preys.

643

644 Finally, it is worth noting that MPS candidates are also significantly enriched in genes related
645 with the immune system. It has been reported that high concentrations of heavy metals
646 negatively affect important processes, such as phagocytosis and chemotaxis, during the
647 generation of the immune response (Boyd, 2010). The footprint of positive selection detected
648 in specialist *Dysdera*, matching phenotypic divergence, might reflect an adaptive mechanism
649 to alleviate the negative immunomodulation effects of heavy metals. In fact, there is evidence
650 that positive selection promoted local adaptation of herbivore insects to heavy metal polluted
651 environments by enhancing immune functions (van Ooik & Rantala, 2010) suggesting the
652 important adaptive character of this system under metal-stress conditions.

653

654 **A possible role of venom toxins in the convergent dietary shift**

655 Stenophagous spiders (e.g., myrmecophagous, termitophagous and araneophagous spiders)
656 show increased venom toxicity to the preferred prey, while related generalists show similar
657 toxicities to all preys (Pekár, Líznavá, Bočánek, & Zdráhal, 2018). The analysis of venom
658 components in stenophagous species indicates that this difference in efficacy is caused by the

659 presence of prey-specific toxins, suggesting evolutionary adaptations for more effective
660 exploitation of focal prey. Notably, we identified a number of transcripts encoding venom
661 toxins among the MGE candidates, most of which were upregulated in specialists, an
662 opposite pattern to that obtained for the rest of the MGE candidates. Among others, we found
663 candidates encoding astacin-like metalloproteases. Astacins share common features with
664 serralysins, matrix metallo-endopeptidases, and snake venom proteases and might be
665 involved in the proteolytic processing of other venom toxins or even play a role in extra-oral
666 digestion of prey, which could be important in the specialization of Canarian *Dysdera* to
667 woodlice. Interestingly, the MGE candidates encoding astacin-like metalloproteases belonged
668 to different orthogroups in each specialist species, which suggests an additional example of
669 functional convergence through different genes. Our analysis also uncovered other candidates
670 that encode some lesser-known toxins, such as products with sequence similarity to U24-
671 ctenitoxin-Pn1a (presumably a protease inhibitor), pisautoxin-Dm1a (a toxin from the venom
672 of the spider *Dolomedes mizhoanus* with an unknown target), alpha-latrotoxins (which induce
673 massive neurotransmitter release) and aranetoxins (also with an unknown target).

674 Remarkably, we found that among the alpha-latrotoxins, a transcript with similarity to a
675 crustacean-selective component of spider venom (the alpha-latrocrustatoxin; Grishin, 1998),
676 also showed the signature of positive selection, making it a promising candidate for
677 stenophagy. Further research including venom gland-specific transcriptomes and the study of
678 venom toxicity to different preys would be required to shed light on the role of venom in the
679 convergent dietary specialization of *Dysdera*.

680

681 **Repeated adaptation to stenophagy in Canarian endemic *Dysdera*: collateral or parallel**
682 **evolution?**

683 Here, we uncovered several pieces of evidence supporting the adaptive divergence hypothesis
684 in stenophagous *Dysdera* inhabiting Western Canary Islands. First, the functional annotation
685 of the majority of genes with concordant changes in gene expression between generalist and
686 specialist spiders clearly points towards an active role of these genes in the dietary shift.
687 Second, we detected repeated episodes of positive selection in the same genes (or
688 functionally related group of genes) in the two specialists' lineages. Furthermore, a
689 significant number of MPS candidates showed convergent amino acid preference shifts in the
690 two focal branches, some of which were also inferred to be under positive selection.
691 Altogether, these results provide new significant evidence that species can find the same
692 molecular solutions to adapt predictably to similar ecological niches more often than
693 previously thought (see Marques et al., 2017; Nosil et al., 2018, for other recent examples).
694
695 Specialist *Dysdera* may have repeatedly adapted to stenophagy through parallel or collateral
696 evolution. In the first case, convergence would result from the accumulation of the same or
697 similar mutations in evolutionary independent lineages, whereas in the second, selection on
698 either shared ancestral or introgressed variations, would be the responsible of the convergent
699 patterns (Stern, 2013). In recent years, increasing evidence has emerged suggesting the
700 important role of shared genetic variation as a substrate for driving repeated evolution of
701 ecotypes in nature (e.g. Jones et al., 2012; Marques, Meier, & Seehausen, 2019; Schluter &
702 Conte, 2009; Van Belleghem et al., 2018). Our genome-wide HRF and D_{FOIL} analyses point
703 to that most of our candidates originated from parallel independent evolution (i.e., relatively
704 low risk of random ILS and non-significant D_{FOIL} results). On the other hand, in the five
705 positive selection candidates where the individual gene trees were incongruent, the apparent
706 homoplasy could be the result of collateral evolution. Unfortunately, in these cases, current
707 data would not allow to disentangle collateral evolution from random ILS at the individual

708 gene level. Accordingly, and to avoid reporting candidates with false patterns of homoplasy,
709 we excluded these five genes with discordant topologies, restricting the analysis on the
710 parallel fixation of *de novo* mutations. Further research including polymorphism from whole
711 genome data would be needed to unequivocally establish the relative role of collateral
712 evolution in the convergence observed in these island endemic spiders.

713

714 Altogether, our findings suggest that the ecological opportunity provided by the colonization
715 of the Canary Islands facilitated the exploration of multiple adaptive landscapes by *Dysdera*
716 and its diversification on similar peaks (Mahler, Ingram, Revell, & Losos, 2013), providing
717 an exceptional example of repeatability in evolution and shedding light on the genetic
718 determinants of phenotypic convergence (Stroud & Losos, 2016). Besides, our results support
719 the idea that convergence can involve repeated changes at different hierarchical levels
720 (Rosenblum, Parent, & Brandt, 2014). We found convergent changes at the amino acid, gene
721 and gene function levels that would be mostly associated to the excretion and detoxification
722 of heavy metals accumulated in the preferred prey, and some venom components likely
723 related with prey capture. We also demonstrated that natural selection promoted the fixation
724 of some of these changes, confirming the view that adaptive forces are a primary determinant
725 of phenotypic convergence (Storz, 2016). Moreover, our report uncovering repeated genetic
726 changes in pairs of phylogenetically-close taxa, supports the ongoing debate that the
727 probability of shared molecular changes for convergent phenotypes correlates with node age
728 (Conte, Arnegard, Peichel, & Schluter, 2012). Hence, this study not only provides new
729 evidence on the genomic basis of an extraordinary example of a convergent ecological shift
730 in a non-model organism but also offers new insights into the longstanding debate about
731 predictability in evolution.

732

733 Acknowledgements

734 We thank to five anonymous reviewers for their useful comments on the manuscript. We also
735 thank Cristina Frías-López for helping with the RNA extractions, and Matthew Hahn for his
736 suggestions and recommendations. This work was supported by the Ministerio de Economía
737 y Competitividad of Spain (CGL2012-36863, CGL2013-45211, CGL2016-75255 and
738 CGL2016-80651) and the Comissió Interdepartamental de Recerca I Innovació Tecnològica
739 of Catalonia, Spain (2014SGR1055 and 2014SGR1604). J.V. was supported by a FPI grant
740 (Ministerio de Economía y Competitividad of Spain, BES-2014-068437). We acknowledge
741 the Cabildos of Tenerife, Gran Canaria and La Gomera, as well as the Garajonay National
742 Park that have granted us collection permits, and often also helped with lodging and logistics
743 during campaigns.
744

745 **References**

- 746 Ahearn, G. A., Sterling, K. M., Mandal, P. K., & Roggenbeck, B. (2010). *Heavy Metal*
747 *Transport and Detoxification by Crustacean Epithelial Lysosomes. Epithelial Transport*
748 *Physiology*. Totowa, NJ: Humana Press.
- 749 Almén, M. S., Lamichhaney, S., Berglund, J., Grant, B. R., Grant, P. R., Webster, M. T., &
750 Andersson, L. (2016). Adaptive radiation of Darwin's finches revisited using whole
751 genome sequencing. *BioEssays*, 38(1), 14–20. doi:10.1002/bies.201500079
- 752 Arnedo, M. (2001). Radiation of the Spider Genus *Dysdera* (Araneae, Dysderidae) in the
753 Canary Islands: Cladistic Assessment Based on Multiple Data Sets. *Cladistics*, 17(4),
754 313–353. doi:10.1006/clad.2001.0168
- 755 Arnedo, M. A., Oromí, P., Múrria, C., Macías-Hernández, N., & Ribera, C. (2007). The dark
756 side of an island radiation: Systematics and evolution of troglobitic spiders of the genus
757 *Dysdera* Latreille (Araneae:Dysderidae) in the Canary Islands. *Invertebrate Systematics*,
758 21(6), 623–660. doi:10.1071/IS07015
- 759 Avise, J. C., & Robinson, T. J. (2008). Hemipecty: A New Term in the Lexicon of
760 Phylogenetics. *Systematic Biology*, 57(3), 503–507. doi:10.1080/10635150802164587
- 761 Bednarska, A. J., Laskowski, R., Pyza, E., Semik, D., Świątek, Z., & Woźnicka, O. (2016).
762 Metal toxicokinetics and metal-driven damage to the gut of the ground beetle
763 *Pterostichus oblongopunctatus*. *Environmental Science and Pollution Research*, 23(21),
764 22047–22058. doi:10.1007/s11356-016-7412-8
- 765 Benjamini, Y. H., & Hochberg, Y. (1995). Controlling The False Discovery Rate - A
766 Practical And Powerful Approach To Multiple Testing. *Journal of the Royal Statistical*
767 *Society*, 57, 289–300. doi:10.2307/2346101
- 768 Boyd, R. S. (2010). Heavy Metal Pollutants and Chemical Ecology: Exploring New
769 Frontiers. *Journal of Chemical Ecology*, 36(1), 46–58. doi:10.1007/s10886-009-9730-5

- 770 Cao, J., & Yan, Q. (2012). Histone Ubiquitination and Deubiquitination in Transcription,
771 DNA Damage Response, and Cancer. *Frontiers in Oncology*, 2, 26.
772 doi:10.3389/fonc.2012.00026
- 773 Chmielowska-Bąk, J., & Deckert, J. (2012). A common response to common danger?
774 Comparison of animal and plant signaling pathways involved in cadmium sensing.
775 *Journal of Cell Communication and Signaling*, 6(4), 191–204. doi:10.1007/s12079-012-
776 0173-3
- 777 Conesa, A., Götz, S., García-Gómez, J. M., Terol, J., Talón, M., & Robles, M. (2005).
778 Blast2GO: a universal tool for annotation, visualization and analysis in functional
779 genomics research. *Bioinformatics*, 21(18), 3674–3676.
780 doi:10.1093/bioinformatics/bti610
- 781 Conte, G. L., Arnegard, M. E., Peichel, C. L., & Schluter, D. (2012). The probability of
782 genetic parallelism and convergence in natural populations. *Proceedings of the Royal
783 Society B: Biological Sciences*, 279(1749), 5039–5047. doi:10.1098/rspb.2012.2146
- 784 Coyne, J. A., & Orr, H. A. (2004). *Speciation*. Sunderland: Sinauer Associates.
- 785 Dejean, A. (1997). Distribution of colonies and prey specialization in the ponerine ant genus
786 *Leptogenys* (Hymenoptera: Formicidae). *Sociobiology*, 29, 293–299.
- 787 Drobne, D. (1997). Terrestrial isopods—a good choice for toxicity testing of pollutants in the
788 terrestrial environment. *Environmental Toxicology and Chemistry*, 16(6), 1159–1164.
789 doi:10.1002/etc.5620160610
- 790 Emerson, B. C. (2002). Evolution on oceanic islands: molecular phylogenetic approaches to
791 understanding pattern and process. *Molecular Ecology*, 11(6), 951–966.
- 792 Falcon, S., & Gentleman, R. (2007). Using GOstats to test gene lists for GO term association.
793 *Bioinformatics*, 23(2), 257–258. doi:10.1093/bioinformatics/btl567
- 794 Fernández, R., Hormiga, G., & Giribet, G. (2014). Phylogenomic Analysis of Spiders

- 795 Reveals Nonmonophyly of Orb Weavers. *Current Biology*, 24(15), 1772–1777.
796 doi:10.1016/j.cub.2014.06.035
- 797 Frías-López, C., Almeida, F. C., Guirao-Rico, S., Vizueta, J., Sánchez-Gracia, A., Arnedo,
798 M. A., & Rozas, J. (2015). Comparative analysis of tissue-specific transcriptomes in the
799 funnel-web spider *Macrothele calpeiana* (Araneae, Hexathelidae). *PeerJ*, 3, e1064.
800 doi:10.7717/peerj.1064
- 801 Gillespie, R. (2004). Community Assembly Through Adaptive Radiation in Hawaiian
802 Spiders. *Science*, 303(5656), 356–359. doi:10.1126/science.1091875
- 803 Gillespie, R. G., & Roderick, G. K. (2002). Arthropods on Islands: Colonization, Speciation,
804 and Conservation. *Annual Review of Entomology*, 47(1), 595–632.
805 doi:10.1146/annurev.ento.47.091201.145244
- 806 Gomes, S. I. L., Scott-Fordsmand, J. J., & Amorim, M. J. B. (2014). Profiling transcriptomic
807 response of *Enchytraeus albidus* to Cu and Ni: Comparison with Cd and Zn.
808 *Environmental Pollution*, 186, 75–82. doi:10.1016/j.envpol.2013.11.031
- 809 Gorvett, H. (1956). Tegumental glands and terrestrial life in woodlice. *Proceedings of the*
810 *Zoological Society of London*, 126(2), 291–314. doi:10.1111/j.1096-
811 3642.1956.tb00439.x
- 812 Grant, P. R., & Grant, B. R. (2008). *How and why species multiply : the radiation of*
813 *Darwin's finches*. Princeton: Princeton University Press.
- 814 Grishin, E. V. (1998). Black widow spider toxins: the present and the future. *Toxicon :*
815 *Official Journal of the International Society on Toxinology*, 36(11), 1693–701.
- 816 Guerrero, R. F., & Hahn, M. W. (2018). Quantifying the risk of hemiplasy in phylogenetic
817 inference. *Proceedings of the National Academy of Sciences of the United States of*
818 *America*, 115(50), 12787–12792. doi:10.1073/pnas.1811268115
- 819 Henning, F., & Meyer, A. (2014). The Evolutionary Genomics of Cichlid Fishes: Explosive

- 820 Speciation and Adaptation in the Postgenomic Era. *Annual Review of Genomics and*
821 *Human Genetics*, 15(1), 417–441. doi:10.1146/annurev-genom-090413-025412
- 822 Hopkin, S. P., & Martin, M. H. (1985). Assimilation of zinc, cadmium, lead, copper, and iron
823 by the spider *Dysdera crocata*, a predator of woodlice. *Bulletin of Environmental*
824 *Contamination and Toxicology*, 34(1), 183–187. doi:10.1007/BF01609722
- 825 Janssens, T. K. S., Roelofs, D., & van Straalen, N. M. (2009). Molecular mechanisms of
826 heavy metal tolerance and evolution in invertebrates. *Insect Science*, 16(1), 3–18.
827 doi:10.1111/j.1744-7917.2009.00249.x
- 828 Jones, F. C., Grabherr, M. G., Chan, Y. F., Russell, P., Mauceli, E., Johnson, J., ... Kingsley,
829 D. M. (2012). The genomic basis of adaptive evolution in threespine sticklebacks.
830 *Nature*, 484(7392), 55–61. doi:10.1038/nature10944
- 831 Juan, C., Emerson, B. C., Oromí, P., & Hewitt, G. M. (2000). Colonization and
832 diversification: towards a phylogeographic synthesis for the Canary Islands. *Trends in*
833 *Ecology & Evolution*, 15(3), 104–109. doi:10.1016/S0169-5347(99)01776-0
- 834 Kanehisa, M., & Goto, S. (2000). KEGG: kyoto encyclopedia of genes and genomes. *Nucleic*
835 *Acids Research*, 28(1), 27–30.
- 836 Köhler, H.-R., & Alberti, G. (1992). The Effect of Heavy Metal Stress on the Intestine of
837 Diplopods. *Berichte Naturwissenschaftlich-Medizinischer Verein Innsbruck*, 10, 257–
838 267.
- 839 Langmead, B., & Salzberg, S. L. (2012). Fast gapped-read alignment with Bowtie 2. *Nature*
840 *Methods*, 9(4), 357–359. doi:10.1038/nmeth.1923
- 841 Lee, J. Y., Yang, J. G., Zhitnitsky, D., Lewinson, O., & Rees, D. C. (2014). Structural basis
842 for heavy metal detoxification by an Atm1-type ABC exporter. *Science*, 343(6175),
843 1133–6. doi:10.1126/science.1246489
- 844 Li, B., & Dewey, C. N. (2011). RSEM: accurate transcript quantification from RNA-Seq data

- 845 with or without a reference genome. *BMC Bioinformatics*, *12*, 323. doi:10.1186/1471-
846 2105-12-323
- 847 Li, C.-C., Wang, Y., Li, G.-Y., Yun, Y.-L., Dai, Y.-J., Chen, J., & Peng, Y. (2016).
848 Transcriptome Profiling Analysis of Wolf Spider *Pardosa pseudoannulata* (Araneae:
849 Lycosidae) after Cadmium Exposure. *International Journal of Molecular Sciences*,
850 *17*(12), 2033. doi:10.3390/ijms17122033
- 851 Li, L., Stoeckert, C. J., & Roos, D. S. (2003). OrthoMCL: identification of ortholog groups
852 for eukaryotic genomes. *Genome Research*, *13*(9), 2178–89. doi:10.1101/gr.1224503
- 853 Losos, J. B., Arnold, S. J., Bejerano, G., Brodie, E. D., Hibbett, D., Hoekstra, H. E., ...
854 Turner, T. L. (2013). Evolutionary Biology for the 21st Century. *PLoS Biology*, *11*(1),
855 e1001466. doi:10.1371/journal.pbio.1001466
- 856 Losos, J. B., & Ricklefs, R. E. (2009). Adaptation and diversification on islands. *Nature*,
857 *457*(7231), 830–836. doi:10.1038/nature07893
- 858 Losos, Jackman, Larson, Queiroz, & Rodriguez-Schettino. (1998). Contingency and
859 determinism in replicated adaptive radiations of island lizards. *Science*, *279*(5359),
860 2115–2118.
- 861 MacArthur, R. H., & Wilson, E. O. (1967). *The Theory of Island Biogeography*. Princeton:
862 Princeton University Press.
- 863 Machado, A., Rodríguez-Expósito, E., López, M., & Hernández, M. (2017). Phylogenetic
864 analysis of the genus *Laparocerus*, with comments on colonisation and diversification in
865 Macaronesia (Coleoptera, Curculionidae, Entiminae). *ZooKeys*, *651*, 1–77.
866 doi:10.3897/zookeys.651.10097
- 867 Macías-Hernández, N., Bidegaray-Batista, L., Emerson, B. C., Oromí, P., & Arnedo, M. A.
868 (2013). The imprint of geologic history on within-island diversification of woodlouse-
869 hunter spiders (Araneae, Dysderidae) in the Canary Islands. *The Journal of Heredity*,

- 870 104(3), 341–356. doi:10.1093/jhered/est008
- 871 Macías-Hernández, N., López, S. de la C., Roca-Cusachs, M., Oromí, P., & Arnedo, M. A.
872 (2016). A geographical distribution database of the genus *Dysdera* in the Canary Islands
873 (Araneae, Dysderidae). *ZooKeys*, (625), 11–23. doi:10.3897/zookeys.625.9847
- 874 Macías-Hernández, N., Oromí, P., & Arnedo, M. A. (2008). Patterns of diversification on old
875 volcanic islands as revealed by the woodlouse-hunter spider genus *Dysdera* (Araneae,
876 Dysderidae) in the eastern Canary Islands. *Biological Journal of the Linnean Society*,
877 94(3), 589–615. doi:10.1111/j.1095-8312.2008.01007.x
- 878 Maddison, W. P. (1997). Gene Trees in Species Trees. *Systematic Biology*, 46(3), 523–536.
879 doi:10.1093/sysbio/46.3.523
- 880 Mahler, D. L., Ingram, T., Revell, L. J., & Losos, J. B. (2013). Exceptional Convergence on
881 the Macroevolutionary Landscape in Island Lizard Radiations. *Science*, 341(6143), 292–
882 295. doi:10.1126/science.1232392
- 883 Marques, D. A., Meier, J. I., & Seehausen, O. (2019). A Combinatorial View on Speciation
884 and Adaptive Radiation. *Trends in Ecology & Evolution*. doi:10.1016/j.tree.2019.02.008
- 885 Marques, D. A., Taylor, J. S., Jones, F. C., Di Palma, F., Kingsley, D. M., & Reimchen, T. E.
886 (2017). Convergent evolution of SWS2 opsin facilitates adaptive radiation of threespine
887 stickleback into different light environments. *PLOS Biology*, 15(4), e2001627.
888 doi:10.1371/journal.pbio.2001627
- 889 Mayr, E. (1942). *Systematics and the Origins of Species*. New York: Columbia University
890 Press.
- 891 Mendes, F. K., Hahn, Y., & Hahn, M. W. (2016). Gene Tree Discordance Can Generate
892 Patterns of Diminishing Convergence over Time. *Molecular Biology and Evolution*,
893 33(12), 3299–3307. doi:10.1093/molbev/msw197
- 894 Mergeay, J., & Santamaria, L. (2012). Evolution and Biodiversity: the evolutionary basis of

- 895 biodiversity and its potential for adaptation to global change. *Evolutionary Applications*,
896 5(2), 103–106. doi:10.1111/j.1752-4571.2011.00232.x
- 897 Merritt, T. J. S., & Bewick, A. J. (2017). Genetic Diversity in Insect Metal Tolerance.
898 *Frontiers in Genetics*, 8, 172. doi:10.3389/fgene.2017.00172
- 899 Migula, P., Wilczek, G., & Babczyńska, A. (2013). *Effects of Heavy Metal Contamination*.
900 *Spider Ecophysiology*. Berlin, Heidelberg: Springer.
- 901 Murrell, B., Wertheim, J. O., Moola, S., Weighill, T., Scheffler, K., & Kosakovsky Pond, S.
902 L. (2012). Detecting Individual Sites Subject to Episodic Diversifying Selection. *PLoS*
903 *Genetics*, 8(7), e1002764. doi:10.1371/journal.pgen.1002764
- 904 Muschick, M., Indermaur, A., & Salzburger, W. (2012). Convergent Evolution within an
905 Adaptive Radiation of Cichlid Fishes. *Current Biology*, 22(24), 2362–2368.
906 doi:10.1016/J.CUB.2012.10.048
- 907 Nelson, D. R., & Nebert, D. W. (2011). *Cytochrome P450 (CYP) Gene Superfamily*.
908 *Encyclopedia of Life Sciences*. Cichester : John Wiley & Sons.
- 909 Norgate, M., Southon, A., Greenough, M., Cater, M., Farlow, A., Batterham, P., ...
910 Camakaris, J. (2010). Syntaxin 5 Is Required for Copper Homeostasis in *Drosophila* and
911 Mammals. *PLoS ONE*, 5(12), e14303. doi:10.1371/journal.pone.0014303
- 912 Nosil, P., Villoutreix, R., de Carvalho, C. F., Farkas, T. E., Soria-Carrasco, V., Feder, J. L.,
913 ... Gompert, Z. (2018). Natural selection and the predictability of evolution in *Timema*
914 stick insects. *Science*, 359(6377), 765–770. doi:10.1126/science.aap9125
- 915 Notredame, C., Higgins, D. G., & Heringa, J. (2000). T-Coffee: A novel method for fast and
916 accurate multiple sequence alignment. *Journal of Molecular Biology*, 302(1), 205–17.
917 doi:10.1006/jmbi.2000.4042
- 918 Paoletti, M. G., & Hassall, M. (1999). Woodlice (Isopoda: Oniscidea): their potential for
919 assessing sustainability and use as bioindicators. *Agriculture, Ecosystems &*

- 920 *Environment*, 74(1–3), 157–165. doi:10.1016/S0167-8809(99)00035-3
- 921 Pease, J. B., & Hahn, M. W. (2015). Detection and Polarization of Introgression in a Five-
922 Taxon Phylogeny. *Systematic Biology*, 64(4), 651–662. doi:10.1093/sysbio/syv023
- 923 Pekár, S., Líznavá, E., & Řezáč, M. (2016). Suitability of woodlice prey for generalist and
924 specialist spider predators: a comparative study. *Ecological Entomology*, 41(2), 123–
925 130. doi:10.1111/een.12285
- 926 Pekár, Stano, Líznavá, E., Bočánek, O., & Zdráhal, Z. (2018). Venom of prey-specialized
927 spiders is more toxic to their preferred prey: A result of prey-specific toxins. *Journal of*
928 *Animal Ecology*, 87(6), 1639–1652. doi:10.1111/1365-2656.12900
- 929 Pond, S. L. K., Frost, S. D. W., & Muse, S. V. (2005). HyPhy: hypothesis testing using
930 phylogenies. *Bioinformatics*, 21(5), 676–679. doi:10.1093/bioinformatics/bti079
- 931 Price, M. N., Dehal, P. S., & Arkin, A. P. (2010). FastTree 2 – Approximately Maximum-
932 Likelihood Trees for Large Alignments. *PLoS ONE*, 5(3), e9490.
933 doi:10.1371/journal.pone.0009490
- 934 Rey, C., Guéguen, L., Sémon, M., & Boussau, B. (2018). Accurate Detection of Convergent
935 Amino-Acid Evolution with PCOC. *Molecular Biology and Evolution*, 35(9), 2296–
936 2306. doi:10.1093/molbev/msy114
- 937 Řezáč, M., & Pekár, S. (2007). Evidence for woodlice-specialization in *Dysdera* spiders:
938 behavioural versus developmental approaches. *Physiological Entomology*, 32(4), 367–
939 371. doi:10.1111/j.1365-3032.2007.00588.x
- 940 Řezáč, M., Pekár, S., & Lubin, Y. (2008). How oniscophagous spiders overcome woodlouse
941 armour. *Journal of Zoology*, 275(1), 64–71. doi:10.1111/j.1469-7998.2007.00408.x
- 942 Robinson, M. D., McCarthy, D. J., & Smyth, G. K. (2010). edgeR: a Bioconductor package
943 for differential expression analysis of digital gene expression data. *Bioinformatics*,
944 26(1), 139–140. doi:10.1093/bioinformatics/btp616

- 945 Roelofs, D., Janssens, T. K. S., Timmermans, M. J. T. N., Nota, B., Mariën, J.,
946 Bochdanovits, Z., ... Van Straalen, N. M. (2009). Adaptive differences in gene
947 expression associated with heavy metal tolerance in the soil arthropod *Orchesella cincta*.
948 *Molecular Ecology*, 18(15), 3227–3239. doi:10.1111/j.1365-294X.2009.04261.x
- 949 Rosenblum, E. B., Parent, C. E., & Brandt, E. E. (2014). The Molecular Basis of Phenotypic
950 Convergence. *Annual Review of Ecology, Evolution, and Systematics*, 45(1), 203–226.
951 doi:10.1146/annurev-ecolsys-120213-091851
- 952 Sánchez-Herrero, J. F., Frías-López, C., Escuer, P., Hinojosa-Alvarez, S., Arnedo, M. A.,
953 Sánchez-Gracia, A., & Rozas, J. (2019). The draft genome sequence of the spider
954 *Dysdera silvatica* (Araneae, Dysderidae): A valuable resource for functional and
955 evolutionary genomic studies in chelicerates. *GigaScience* (accepted).
- 956 Sanderson, M. J. (2003). r8s: inferring absolute rates of molecular evolution and divergence
957 times in the absence of a molecular clock. *Bioinformatics*, 19(2), 301–302.
958 doi:10.1093/bioinformatics/19.2.301
- 959 Sanderson, Michael J. (2002). Estimating absolute rates of molecular evolution and
960 divergence times: a penalized likelihood approach. *Molecular Biology and Evolution*,
961 19(1), 101–9.
- 962 Schieber, M., & Chandel, N. S. (2014). ROS function in redox signaling and oxidative stress.
963 *Current Biology : CB*, 24(10), R453-462. doi:10.1016/j.cub.2014.03.034
- 964 Schluter, D. (2000). *The ecology of adaptive radiation*. Oxford: Oxford Univ. Press, Oxford.
- 965 Schluter, D., & Conte, G. L. (2009). Genetics and ecological speciation. *Proceedings of the*
966 *National Academy of Sciences of the United States of America*, 106 Suppl 1(Supplement
967 1), 9955–62. doi:10.1073/pnas.0901264106
- 968 Schmalzfuss, H. (1984). Eco-morphological strategies in terrestrial isopods. *Symposium of the*
969 *Zoological Society of London*, 53, 49–63.

- 970 Smith, M. D., Wertheim, J. O., Weaver, S., Murrell, B., Scheffler, K., & Kosakovsky Pond,
971 S. L. (2015). Less Is More: An Adaptive Branch-Site Random Effects Model for
972 Efficient Detection of Episodic Diversifying Selection. *Molecular Biology and*
973 *Evolution*, 32(5), 1342–1353. doi:10.1093/molbev/msv022
- 974 Sooksa-Nguan, T., Yakubov, B., Kozlovskyy, V. I., Barkume, C. M., Howe, K. J.,
975 Thannhauser, T. W., ... Vatamaniuk, O. K. (2009). *Drosophila* ABC transporter,
976 DmHMT-1, confers tolerance to cadmium. DmHMT-1 and its yeast homolog, SpHMT-
977 1, are not essential for vacuolar phytochelatin sequestration. *The Journal of Biological*
978 *Chemistry*, 284(1), 354–62. doi:10.1074/jbc.M806501200
- 979 Stamatakis, A. (2014). RAxML version 8: a tool for phylogenetic analysis and post-analysis
980 of large phylogenies. *Bioinformatics*, 30(9), 1312–3. doi:10.1093/bioinformatics/btu033
- 981 Stern, D. L. (2013). The genetic causes of convergent evolution. *Nature Reviews Genetics*,
982 14(11), 751–764. doi:10.1038/nrg3483
- 983 Storz, J. F. (2016). Causes of molecular convergence and parallelism in protein evolution.
984 *Nature Reviews Genetics*, 17(4), 239–250. doi:10.1038/nrg.2016.11
- 985 Stroud, J. T., & Losos, J. B. (2016). Ecological Opportunity and Adaptive Radiation. *Annual*
986 *Review of Ecology, Evolution, and Systematics*, 47(1), 507–532. doi:10.1146/annurev-
987 ecolsys-121415-032254
- 988 Supek, F., Bošnjak, M., Škunca, N., & Šmuc, T. (2011). REVIGO summarizes and visualizes
989 long lists of gene ontology terms. *PloS One*, 6(7), e21800.
990 doi:10.1371/journal.pone.0021800
- 991 Sutton, S. L. (1980). *Woodlice*. New York: Pergamon Press.
- 992 Toft, S., & Macías-Hernández, N. (2017). Metabolic adaptations for isopod specialization in
993 three species of *Dysdera* spiders from the Canary Islands. *Physiological Entomology*,
994 42(2), 191–198. doi:10.1111/phen.12192

- 995 Van Belleghem, S. M., Vangestel, C., De Wolf, K., De Corte, Z., Möst, M., Rastas, P., ...
996 Hendrickx, F. (2018). Evolution at two time frames: Polymorphisms from an ancient
997 singular divergence event fuel contemporary parallel evolution. *PLOS Genetics*, *14*(11),
998 e1007796. doi:10.1371/journal.pgen.1007796
- 999 van Ooik, T., & Rantala, M. J. (2010). Local Adaptation of an Insect Herbivore to a Heavy
1000 Metal Contaminated Environment. *Annales Zoologici Fennici*, *47*(3), 215–222.
1001 doi:10.5735/086.047.0306
- 1002 Van Straalen, N. M., & Roelofs, D. (2005). Cadmium tolerance in a soil arthropod a model of
1003 real-time microevolution. *Entomologische Berichten*, *65*(4), 105–111.
- 1004 Vizuela, J., Frías-López, C., Macías-Hernández, N., Arnedo, M. A., Sánchez-Gracia, A., &
1005 Rozas, J. (2017). Evolution of chemosensory gene families in arthropods: Insight from
1006 the first inclusive comparative transcriptome analysis across spider appendages. *Genome*
1007 *Biology and Evolution*, *9*(1), 178–196. doi:10.1093/gbe/evw296
- 1008 Vizuela, J., Rozas, J., & Sánchez-Gracia, A. (2018). Comparative Genomics Reveals
1009 Thousands of Novel Chemosensory Genes and Massive Changes in Chemoreceptor
1010 Repertoires across Chelicerates. *Genome Biology and Evolution*, *10*(5), 1221–1236.
1011 doi:10.1093/gbe/evy081
- 1012 Wertheim, J. O., Murrell, B., Smith, M. D., Kosakovsky Pond, S. L., & Scheffler, K. (2015).
1013 RELAX: detecting relaxed selection in a phylogenetic framework. *Molecular Biology*
1014 *and Evolution*, *32*(3), 820–832. doi:10.1093/molbev/msu400
- 1015 Whittaker, R. J., & Fernández-Palacios, J. M. (2007). *Island biogeography: ecology,*
1016 *evolution, and conservation*. Oxford: Oxford Univ. Press.
- 1017 Wilczek, G., Babczyńska, A., Migula, P., & Wencelis, B. (2003). Activity of Esterases as
1018 Biomarkers of Metal Exposure in Spiders from the Metal Pollution Gradient. *Polish*
1019 *Journal of Environmental Studies*, *12*(6), 765–771.

- 1020 World Spider Catalog. (2019). World Spider Catalog. Version 20.0. *Natural History Museum*
1021 *Bern*, online at <http://wsc.nmbe.ch>. doi:10.24436/2
- 1022 Wu, M., Kostyun, J. L., Hahn, M. W., & Moyle, L. C. (2018). Dissecting the basis of novel
1023 trait evolution in a radiation with widespread phylogenetic discordance. *Molecular*
1024 *Ecology*, 27(16), 3301–3316. doi:10.1111/mec.14780
- 1025 Zapata, M., Tanguy, A., David, E., Moraga, D., & Riquelme, C. (2009). Transcriptomic
1026 response of *Argopecten purpuratus* post-larvae to copper exposure under experimental
1027 conditions. *Gene*, 442(1–2), 37–46. doi:10.1016/J.GENE.2009.04.019
- 1028 Zhang, C., Rabiee, M., Sayyari, E., & Mirarab, S. (2018). ASTRAL-III: polynomial time
1029 species tree reconstruction from partially resolved gene trees. *BMC Bioinformatics*,
1030 19(S6), 153. doi:10.1186/s12859-018-2129-y
- 1031 Zhang, Y., Lambiase, S., Fasola, M., Gandini, C., Grigolo, A., & Laudani, U. (2001).
1032 Mortality and tissue damage by heavy metal contamination in the German cockroach,
1033 *Blattella germanica* (Blattaria, Blattellidae). *Italian Journal of Zoology*, 68(2), 137–145.
1034 doi:10.1080/11250000109356398
- 1035

1036 Authors' contributions

1037 A.S-G. and J.R. designed, conceived and supervised the research; N.M-H and M.A.A.
1038 provided the biological material. J.V. performed the experiments and the bioinformatics
1039 work, and analysed the data. M.A.A. performed the dissecting analysis and participated in the
1040 data interpretation. J.V., J.R. and A.S-G. wrote the first version of the manuscript. N.M-H.
1041 and M.A.A. revised the manuscript and participated in the writing of the final version. All
1042 authors read and approved the final version of the manuscript.

1043

1044 Data accessibility

1045 The raw sequence data generated for this work has been deposited at the Sequence Read
1046 Archive (SRA) under Bioproject PRJNA437566. Additional data and analysis generated in
1047 this study have been deposited in Figshare (<https://doi.org/10.6084/m9.figshare.7726508.v1>).

1048

1049 Competing interests

1050 The authors declare that they have no competing interests

1051

1052 **Figures**

1053

1054 **Figure 1. a.** Map of the Canary Islands showing the geographic location of capture localities.1055 **b.** Phylogenetic relationships and divergence times (scale bar) among surveyed *Dysdera*1056 species. The continental species *D. crocata* was used to root the tree. **c.** Dissecting scope1057 images of the left chelicera: A-B: *Dysdera silvatica* female, La Gomera, A, ventral view; B,1058 lateral view; C-D: *D. verneaui* female, Tenerife, C, ventral view, D, lateral view; E-F: *D.*1059 *bandamae* female, Gran Canaria, E, ventral view, F, lateral view; G-H: *D. gomerensis*1060 female, La Gomera, G, ventral view, H, lateral view; I-J: *D. tilosensis* male, Gran Canaria, I,

1061 lateral view, J, lateral view. Bars indicate the relative lengths of the different parts of the

1062 chelicerae to highlight differences between the standard (generalists) and elongated or

1063 slightly elongated (specialists) chelicerae. White bar: total length of the basal segment (b),

1064 dotted part: length of the cheliceral groove (g). Black bar: length of the cheliceral fang (f). In

1065 standard chelicerae, g is approximately 1/3 of b, and f is similar to the distance between the

1066 base of the segment and the end of the internal keel (k), while in elongated chelicerae, g is

1067 longer than 2/5 of f, and f is longer than k. Scale bar in mm. **d.** Live images of the target1068 *Dysdera* species; photo credit: Pedro Oromí.

1069

1070 **Figure 2.** Core analyses workflow applied in this study, including a summary of the most

1071 relevant results. DE, differential expression; DFC, differential functional constraints; PS,

1072 positive selection; *, patterns matching the observed phenotypic convergence.

1073

1074 **Figure 3.** Species tree inferred with Astral showing the risk of hemiplasy along the

1075 phylogeny. Hemiplasy risk factor values (HRF) were estimated for all internal branches of

1076 the tree. The relative probabilities of hemiplasy and homoplasy were inferred under different

1077 effective population sizes (N_e ; panels **a** to **d**) and assuming a fixed mutation rate μ per $2N_e$
1078 generations ($2N_e\mu = 5.5 \times 10^{-3}$). HRF values estimated for all internal branches (in brackets)
1079 represent the proportion of discordant traits associated with a branch due to hemiplasy.

1080

1081 **Figure 4.** Heat map with body part-specific gene expression profiles of the 144 MGE
1082 candidates.

1083

1084 **Figure 5.** Bar charts with the most relevant results of the GO enrichment analyses (see Figure
1085 S3 for more detailed versions). **a.** Orthogroups with differential expression profiles matching
1086 phenotypic convergence (144 MGE candidates) **b.** Orthogroups under positive selection in
1087 the two specialists (17 MPS candidates) **c.** Most representative candidates encoding venom
1088 toxins in stenophagous *Dysdera*. Dark and light tones represent the proportion of genes with
1089 a given associated GO in the candidate and the population (whole transcriptome) set,
1090 respectively.

1091

1092 **Figure 6.** Relevant orthogroups showing evidence of convergent amino acid substitutions. (**a**)
1093 orthogroup encoding the venom toxin OG6752. (**b-f**) orthogroups with positions evolving
1094 under positive selection. Amino acid positions are shaded with different tones according to
1095 their profiles, and only positions with a PP equal to or greater than 0.99 according to the
1096 PCOC, PC or OC model are shown (Rey et al., 2018). Stars highlight the sites identified as
1097 being positively selected in MEME.

1098

1099

1100 **Tables**

1101 **Table 1.** Summary of dietary habits, sampling localities, RNA-seq data and assembly
1102 statistics for each surveyed *Dysdera* species.

1103

1104

1105

Supplementary material

1106

Supplementary figures

1108

1109 **Figure S1.** Distribution of blastx hits across species. Distribution of the top 5 hits from the
1110 blastx searches with the transcripts of each *Dysdera* species against the ArthropodDB
1111 database.

1112

1113 **Figure S2.** Principal component analysis (PCA) of gene expression profiles of individual
1114 *REST* samples from *D. tilosensis*.

1115

1116 **Figure S3.** Venn diagrams showing (a) the number of shared genes between species pairs.
1117 Differential expressed (DE) genes are showed in brackets; (b) the number of DE genes
1118 between species pairs and groups of tissues (*LEGS-PALP* refers to the *LEG#1*, *LEG#234* and
1119 *PALP*); (c) number of MGE candidates across tissues.

1120

1121 **Figure S4.** Tree maps with detailed GO enrichment results generated with REVIGO.

1122

1123 **Figure S5.** Box plots showing the distribution of ω values for all single-copy orthogroups in
1124 specialist (orange) and generalist (blue) species.

1125

1126 **Figure S6.** Orthogroups with evidence of convergent amino acid evolution. Amino acid
1127 positions are coloured according to their profiles, and only positions with a *PP* equal to or
1128 greater than 0.99 according to the PCOC, PC or OC model are shown. Yellow stars highlight
1129 the sites identified as positively selected in MEME.

1130

1131

1132 **Supplementary tables**

1133 **Table S1.** RNA-seq statistics.

1134

1135 **Table S2.** Distribution of the percentage of CEG length covered by blastx hits.

1136

1137 **Table S3.** Orthogroups classification.

1138

1139 **Table S4.** List of genes with concordant differential expression profiles between generalist
1140 and specialists species.

1141

1142 **Table S5.** List of genes with concordant differential functional constraint profiles between
1143 generalist and specialist species.

1144

1145 **Table S6.** List of genes with concordant signals of positive selection in specialist species.

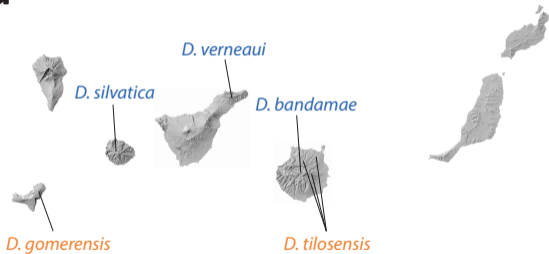
1146

1147 **Supplementary methods**

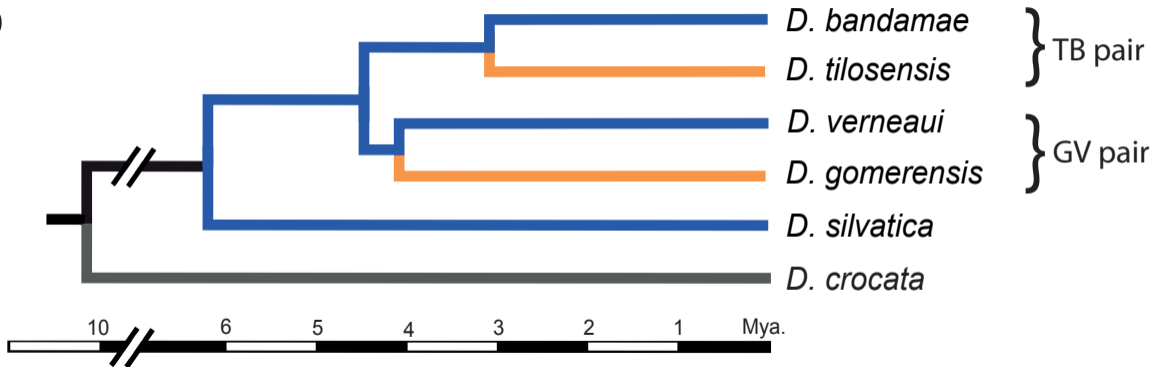
1148 Supplementary Information of transcriptome, differential gene expression and selective
1149 constraint analyses.

1150

a



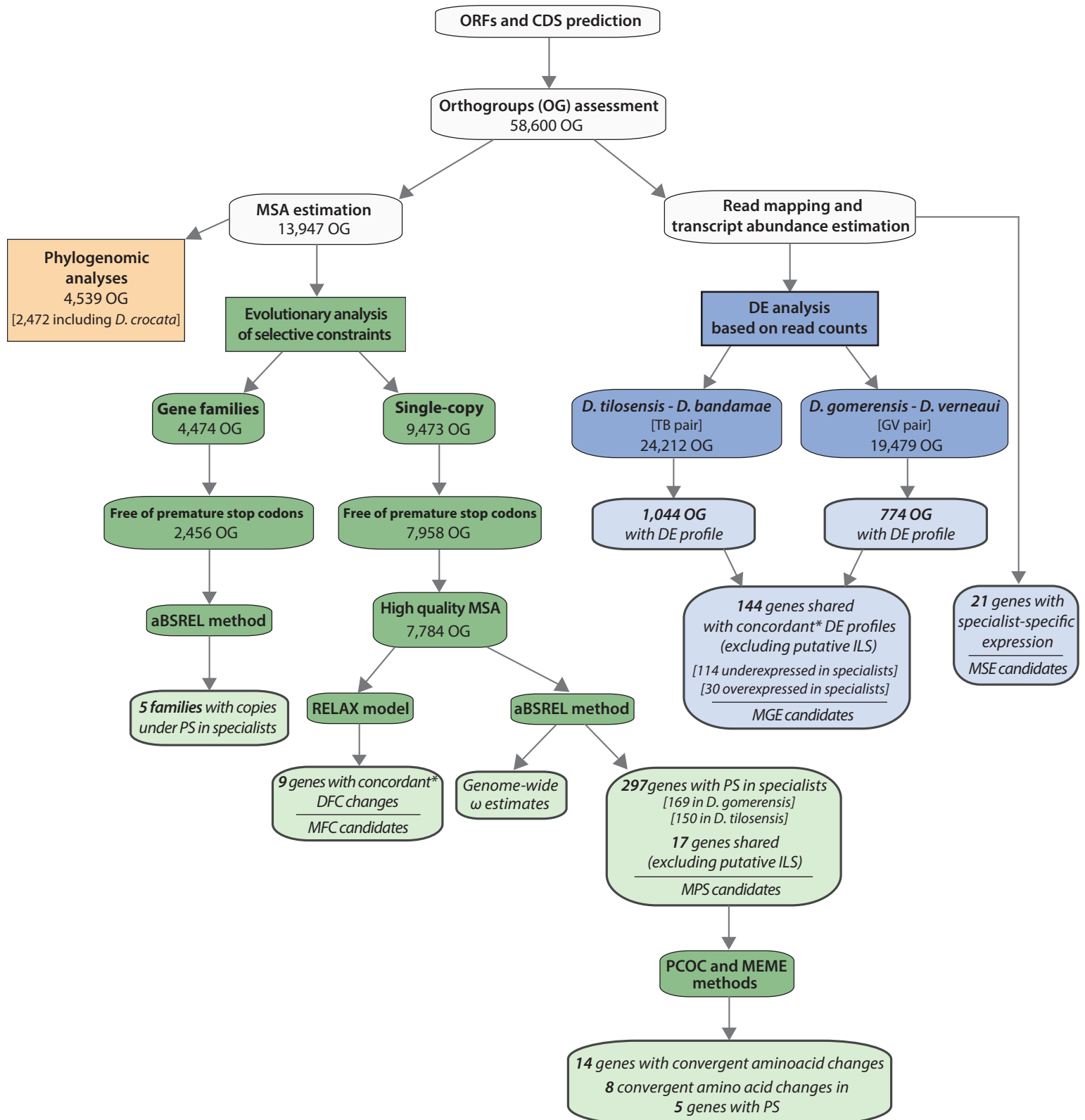
Molecular Ecology

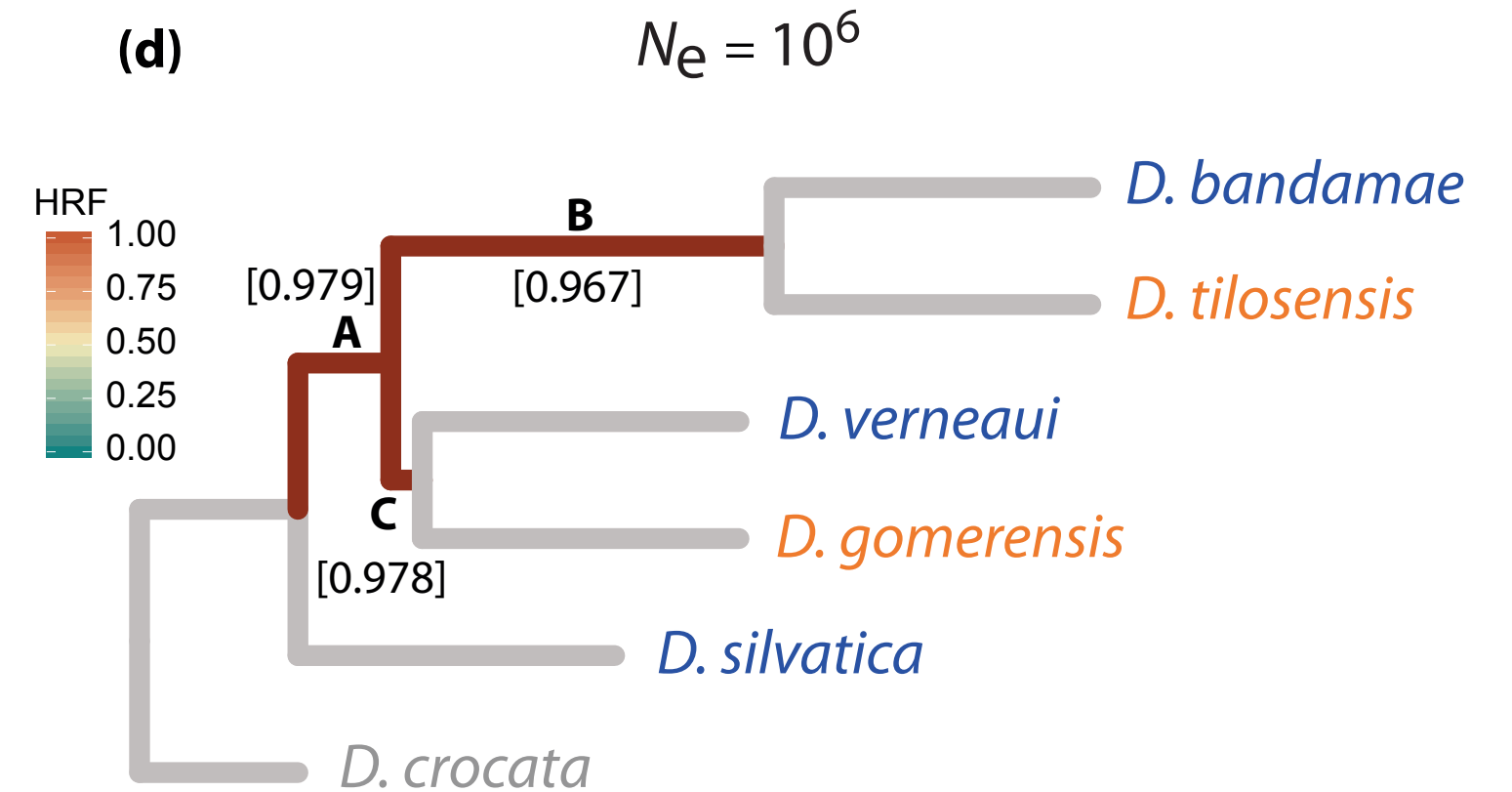
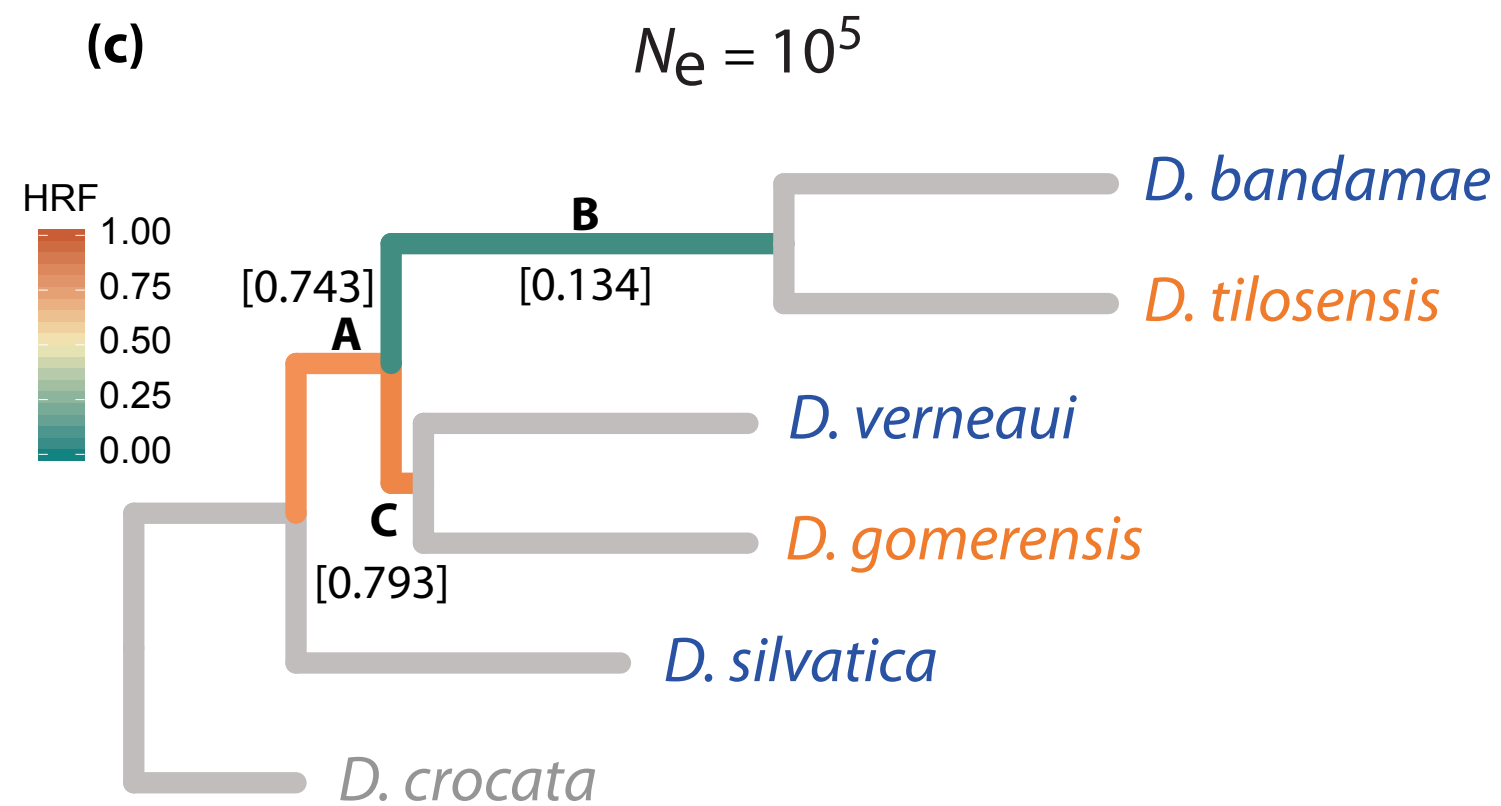
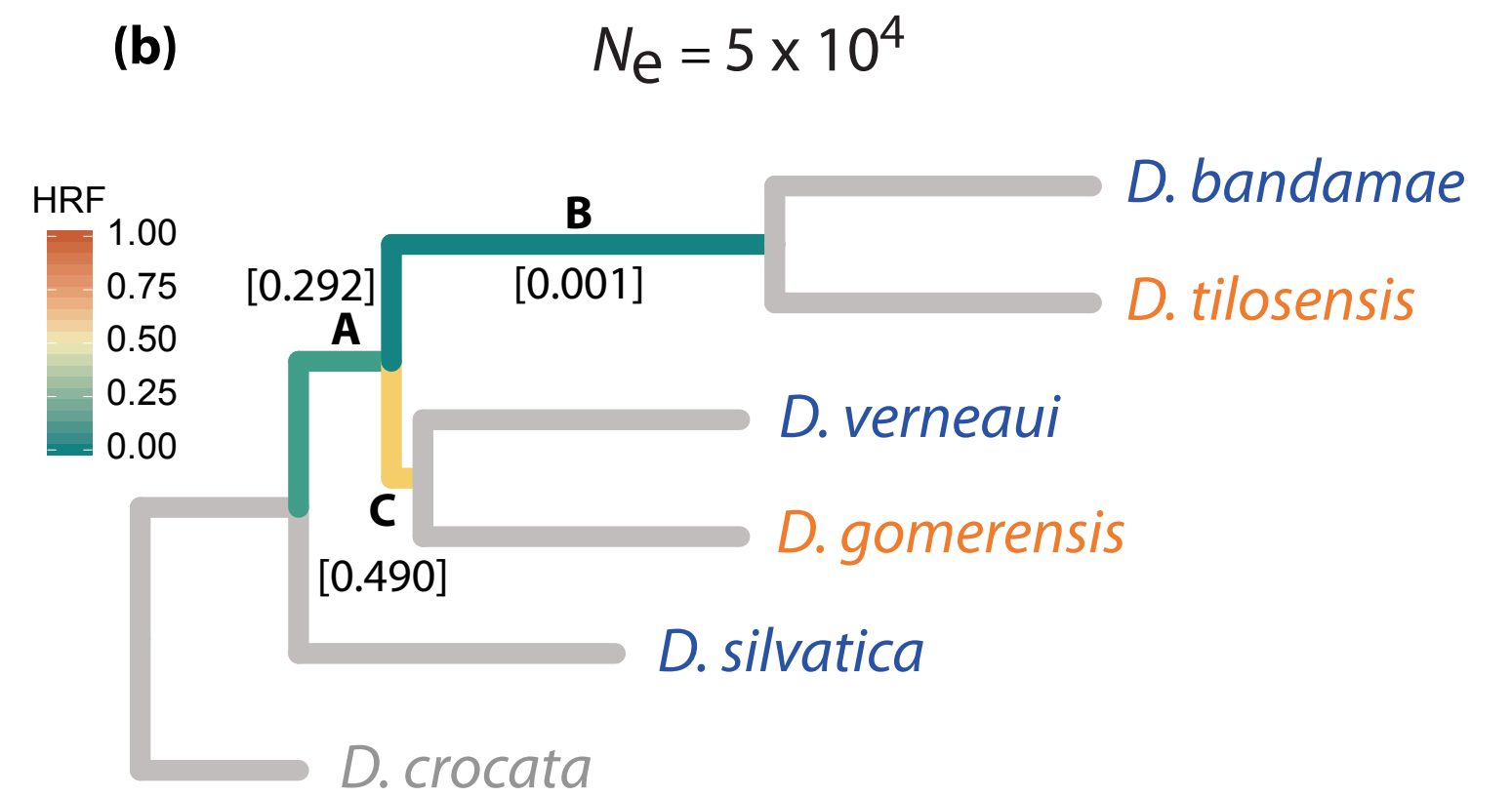
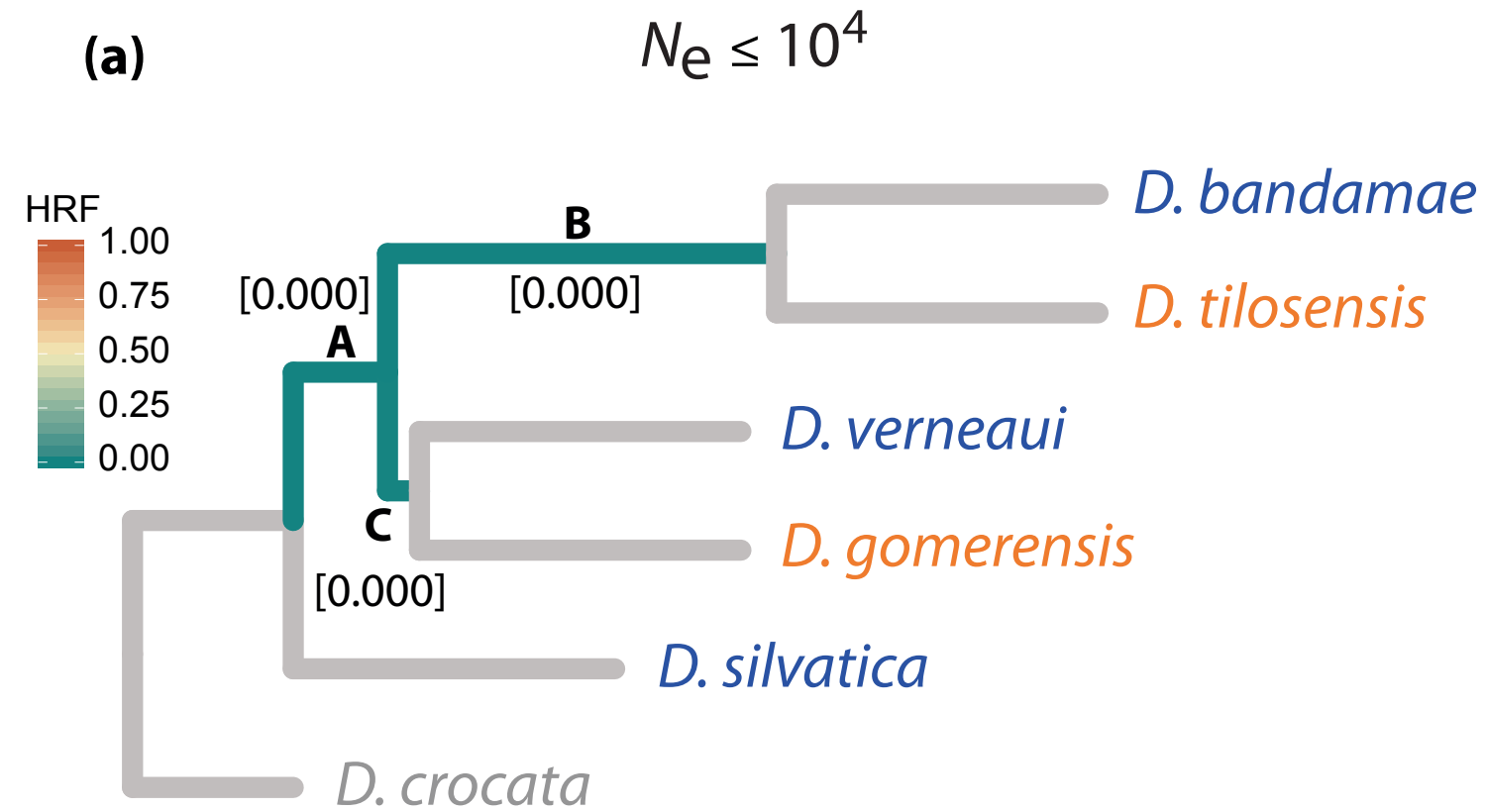
b

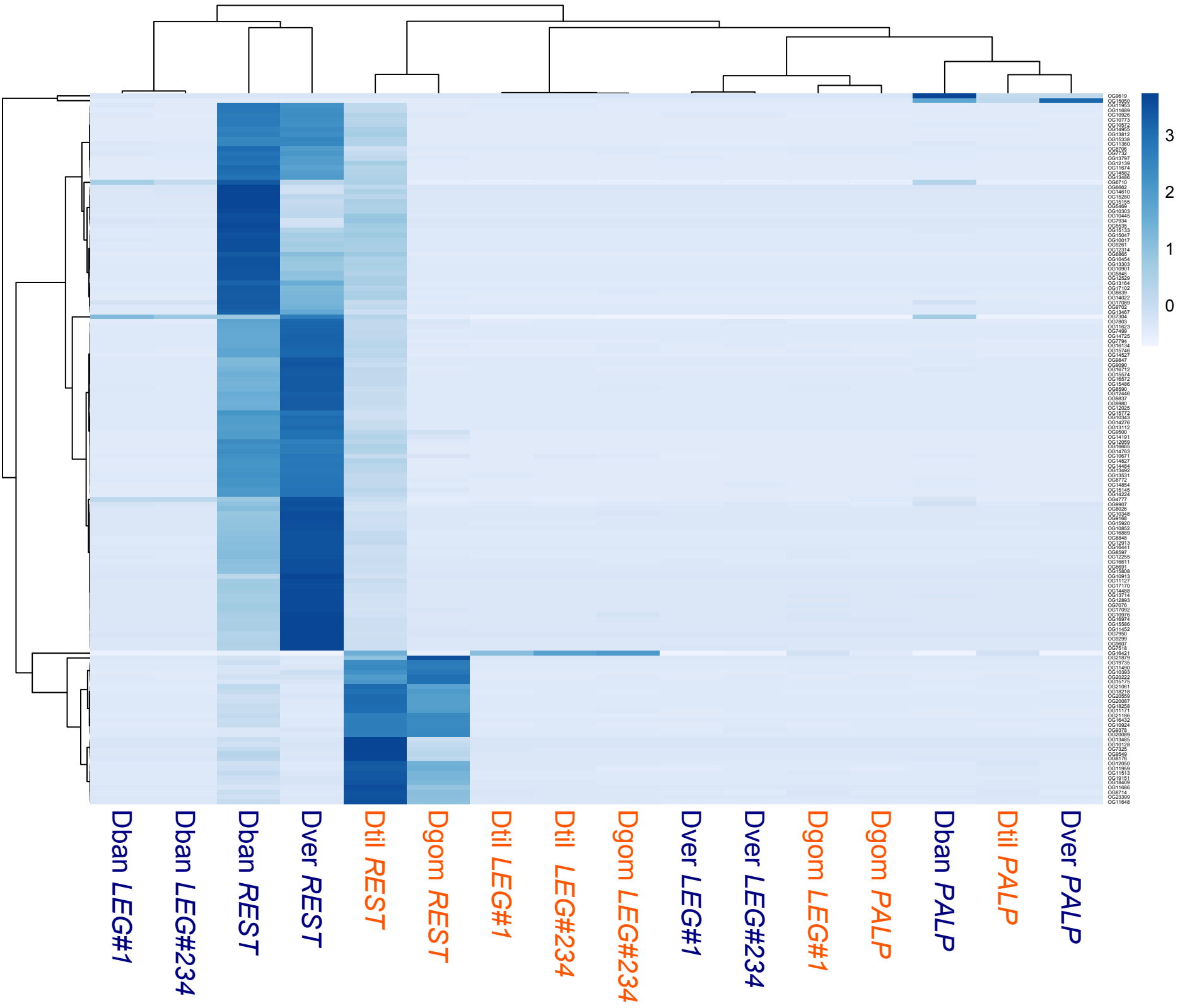
Unable to Convert Image

The dimensions of this image (in pixels) are too large to be converted. For this image to convert, the total number of pixels (height x width) must be less than 40,000,000 (40 megapixels).

Figure 1cd





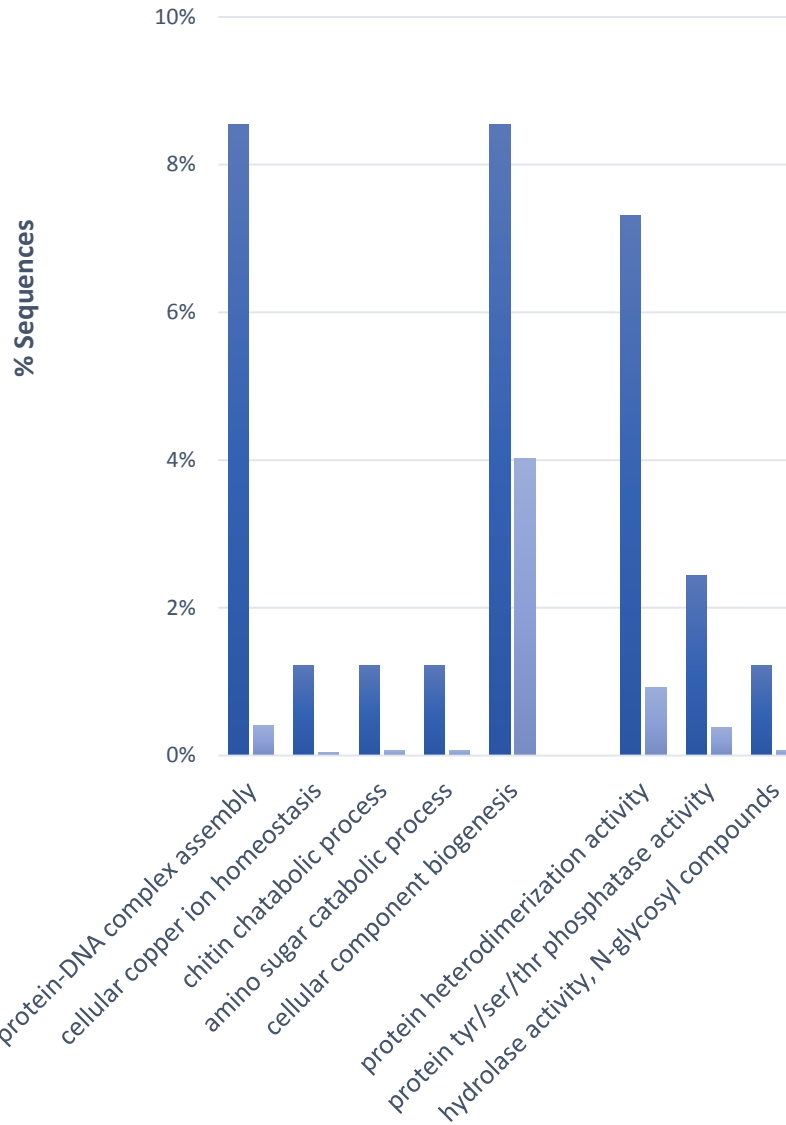


a

MGE candidates

Biological process

Molecular Function



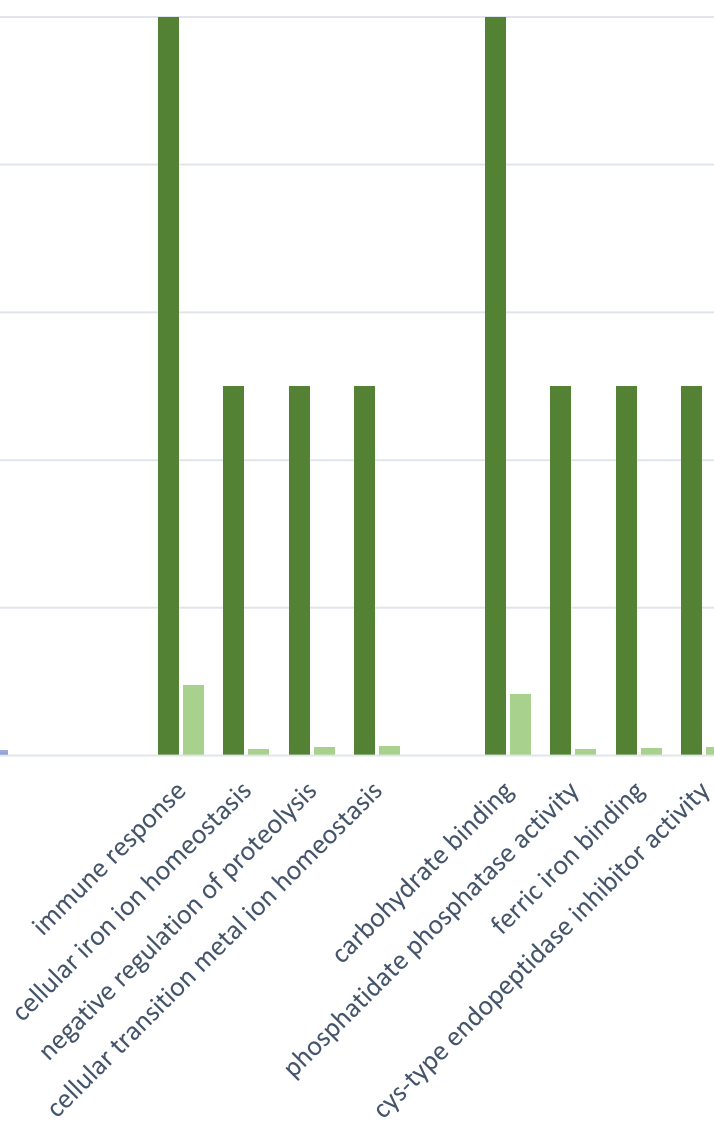
b

Molecular Ecology

MPS candidates

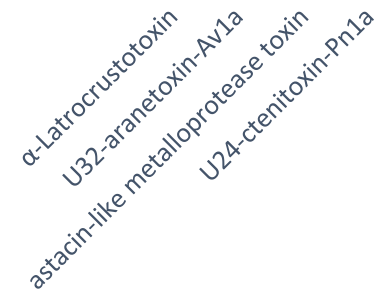
Biological process

Molecular Function



c

Candidate toxins



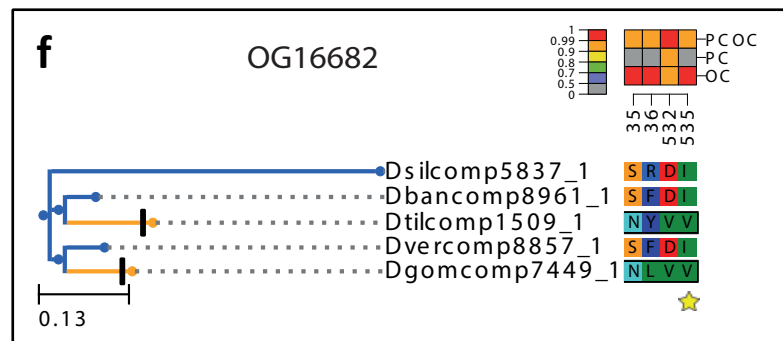
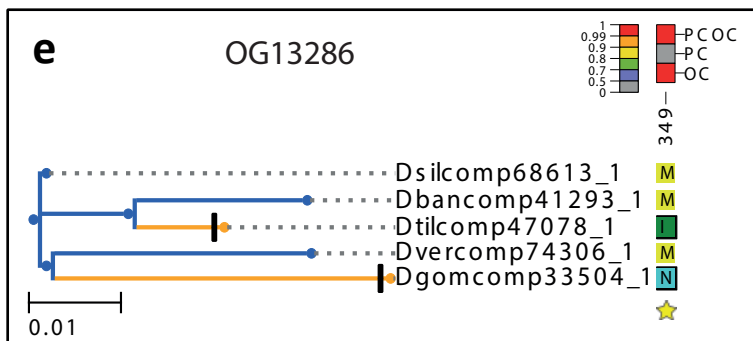
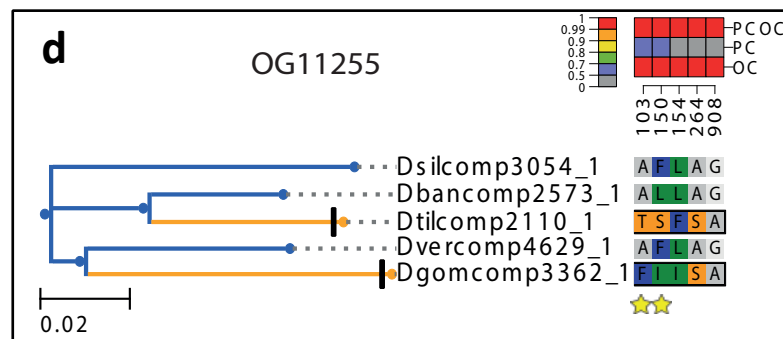
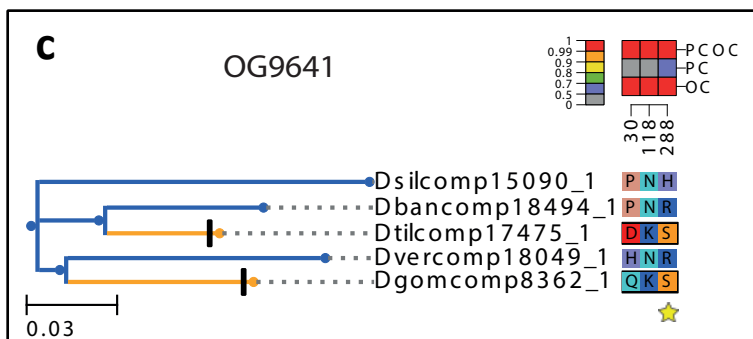
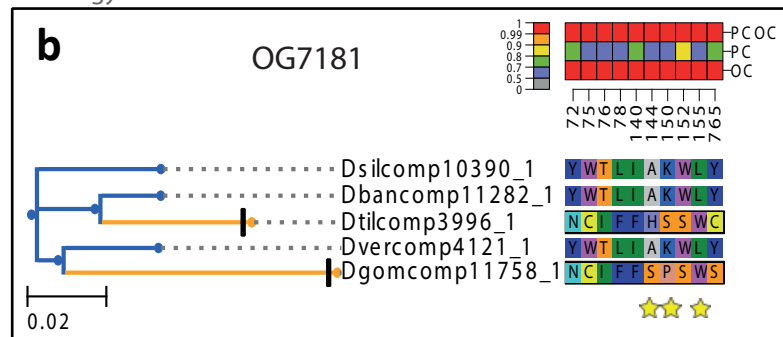
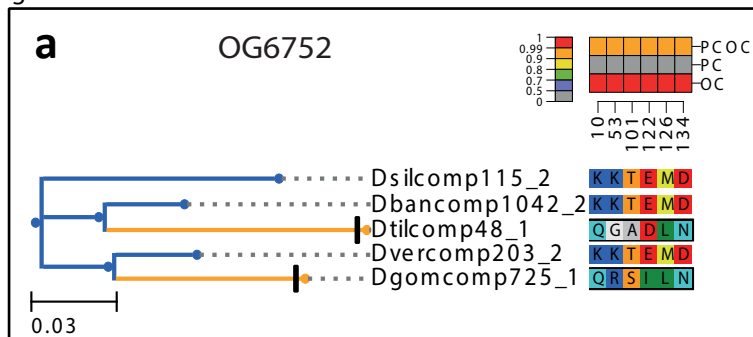


Table 1. Summary of dietary habits, sampling localities, RNA-seq data and assembly statistics for each surveyed *Dysdera* species

	<i>D. silvatica</i>	<i>D. verneui</i>	<i>D. gomerensis</i>	<i>D. bandamae</i>	<i>D. tilosensis</i>
Diet	Generalist	Generalist	Specialist	Generalist	Specialist
Locality (in Canary Island)	La Gomera	Tenerife	El Hierro	Gran Canaria	Gran Canaria
Total raw reads	441,835,864	527,299,202	430,522,240	765,653,462	678,150,384
Total qualified reads	418,205,054	495,937,054	400,095,710	746,925,920	664,654,842
Transcripts	236,283	441,604	213,984	296,544	316,498
Genes (clustered isoforms)	170,846	347,878	177,363	221,801	229,762
Gene average length (in bp)	702	525	622	658	649
Gene maximum length (in bp)	26,709	27,235	27,386	27,369	25,342
HK genes	1,136	1,194	1,232	1,153	1,159
CEG genes	807 (457)	1,180 (457)	1,111 (457)	1,033 (457)	1,143 (457)
GO annotated genes	29,879	38,361	28,158	35,116	37,246
Genes with InterPro domain	30,886	40,771	29,930	37,413	39,480
Functional annotated genes ^a	31,091	41,019	30,106	37,620	39,704
Annotated genes ^b	41,046	51,864	37,087	47,059	50,150
Predicted coding sequences (CDS)	58,966	84,114	55,914	72,352	77,756
% not coding genes	34.51%	24.18%	31.53%	32.62%	33.84%
% not annotated CDS	69.61%	61.66%	66.33%	65.04%	64.50%
1to1 orthologs in all species	9,473	9,473	9,473	9,473	9,473
1to1 orthologs per species pair	-	19,497	19,497	24,212	24,212

^aGO or Interpro hits.

^bGO, Interpro or blast hits.